Quaternary Science Reviews 375 (2026) 109777

Contents lists available at ScienceDirect

Quaternary Science Reviews

journal homepage: www.elsevier.com/locate/quascirev

# A tale of two regions: Cyclical human-climate interactions in the South Levant from the Chalcolithic to the Iron Age (6500–2200 BP)

Andrea Titolo *, Alessio Palmisano

*University of Turin, Department of Historical Studies, Palazzo Nuovo, Via S. Ottavio, 20, 10124, Torino, Italy*

ARTICLE INFO

Handling Editor: Donatella Magri

*Keywords:*
Paleodemography
Multi-proxy approach
Radiocarbon summed probability distribution
Archaeological survey
Speleothem
Paleoclimate
South levant

ABSTRACT

This paper investigates long-term trends in human population and their relationship with climate in two sub-regions of the South Levant (here labelled Samaria and Judah) from the Chalcolithic to the end of Iron Age III (6500-2200 cal yr BP). We aim to reconstruct demographic fluctuations and the sub-regional level, evaluate possible cycles of climate-population relations, to understand if different scales of analyses can reveal more nuanced population variations than what is already known for the whole South Levant, and to tackle a current debate on the Iron Age II dynamics in the region. To do so, we employ a multi-proxy approach with a carefully crafted dataset composed of radiocarbon dates, archaeological sites from published surveys and excavations, and well-known paleoclimate proxies (n = 4), which were analysed through a suite of mature statistical and quantitative techniques. More specifically, we employed probabilistic approaches, entailing SPDs generation, Aoristic techniques, Monte Carlo simulations, and moving-window techniques to answer questions of long-term population changes and their relation to climate. Our results show that a multi-scalar approach can reveal interesting patterns that add significant details to regional reconstructions, with the two regions following similar patterns but each dependent on the geographical, socio-political, and economic context of the area in each period. We highlighted cycles of climate-population nexus, evidence of societal resilience and population overshoot, and larger climatic impact on population in desert fringe areas, although maintaining that climate alone cannot be taken as the sole explanatory factor for population fluctuations. We also provided a more nuanced interpretation of the Iron Age II dynamics beyond the simple juxtaposition of desolation and prosperity related to the Assyrian domination, which can now be evaluated without the risk of misinterpretations due to the partial use of just archaeological excavation data.

## 1. Introduction

Over the last decade, a growing literature emphasised how multi-proxy approaches are best suited for modelling and reconstructing long-term demographic trends (Crema et al. 2016; Crema and Kobayashi 2020; Feeser et al. 2019; French 2015; Lawrence et al. 2021; Palmisano et al. 2017, 2021b; *2019*; Tallavaara and Pesonen 2020). These approaches leveraged the widespread archaeological radiocarbon databases at the regional/national scale or at the global scale (Bird et al. 2022; Bronk Ramsey et al. 2019; e.g. Capriles 2023; Hinz et al. 2012; Hoggarth et al. 2021; Katsianis et al. 2020; Kelly et al. 2022; Kudo et al. 2023; Loftus et al. 2019; Lucarini et al. 2020; Palmisano et al., 2022a; Palmisano et al. 2022b; Pardo-Gordó et al. 2023; Petchey et al. 2022; Rademaker 2024; Roe et al. 2025; Schmid et al. 2019), a growing availability of archaeological data from online databases or specific projects (albeit still a limited practice, Batist and Roe 2024; Palmisano and Titolo 2024), and a now mature suite of statistical and quantitative methods for overcoming intrinsic data limitations (Bevan and Crema 2020; Bronk Ramsey 2017; Brown 2017; Crema et al. 2016; Crema 2022; Crema and Shoda 2021; McLaughlin 2019; Palmisano 2023; Timpson et al. 2014, *2020*). These approaches have the advantage of moving beyond the simple concept of *dates-as-data* (Rick 1987), to combine datasets with different temporal resolution and interpretative potential, and offering a more compelling understanding of past population dynamics by cross-checking demographic curves and assessing their overlap and robustness (Roberts 2021). For inferring past population dynamics, together with radiocarbon dates, the most commonly used proxies are raw counts of archaeological sites and, when available, estimated settlement size (French et al. 2021; Palmisano et al. 2021a). Generally speaking, inferring population dynamics and demographic

* Corresponding author.
*E-mail address:* andrea.titolo@unito.it (A. Titolo).

https://doi.org/10.1016/j.quascirev.2025.109777
Received 30 September 2025; Received in revised form 18 December 2025; Accepted 21 December 2025
Available online 2 January 2026

trends for past societies is based on the assumption that, in a given study area, a direct linear relationship exists between the density of archaeological evidence and its past population (i.e. the larger the past population, the more archaeological evidence will be recovered from surveys and excavations, Drennan et al. 2015). Of course, both archaeological and radiocarbon data suffer from different limitations related to visibility, sampling, measurement errors, etc., which render this equation dangerous if taken for granted (see Crema 2022; Palmisano 2023; Tallavaara and Jørgensen 2020) (see also *paragraph 2.4* below). Moreover, an important clarification to make is that the resulting demographic curves do not offer evidence for absolute numbers of people in the past, but rather they provide a relative measure of intensities and changes through time.

Developments in archaeological demographic studies fit in the framework of a revitalised interest in the relationship between archaeological demography and social complexity, climate change, and historical events (e.g. Cookson et al. 2019; Kaniewski et al. 2019; Kolář et al. 2022; Lawrence et al. 2022; Marchetti et al. 2025; Palmisano et al.

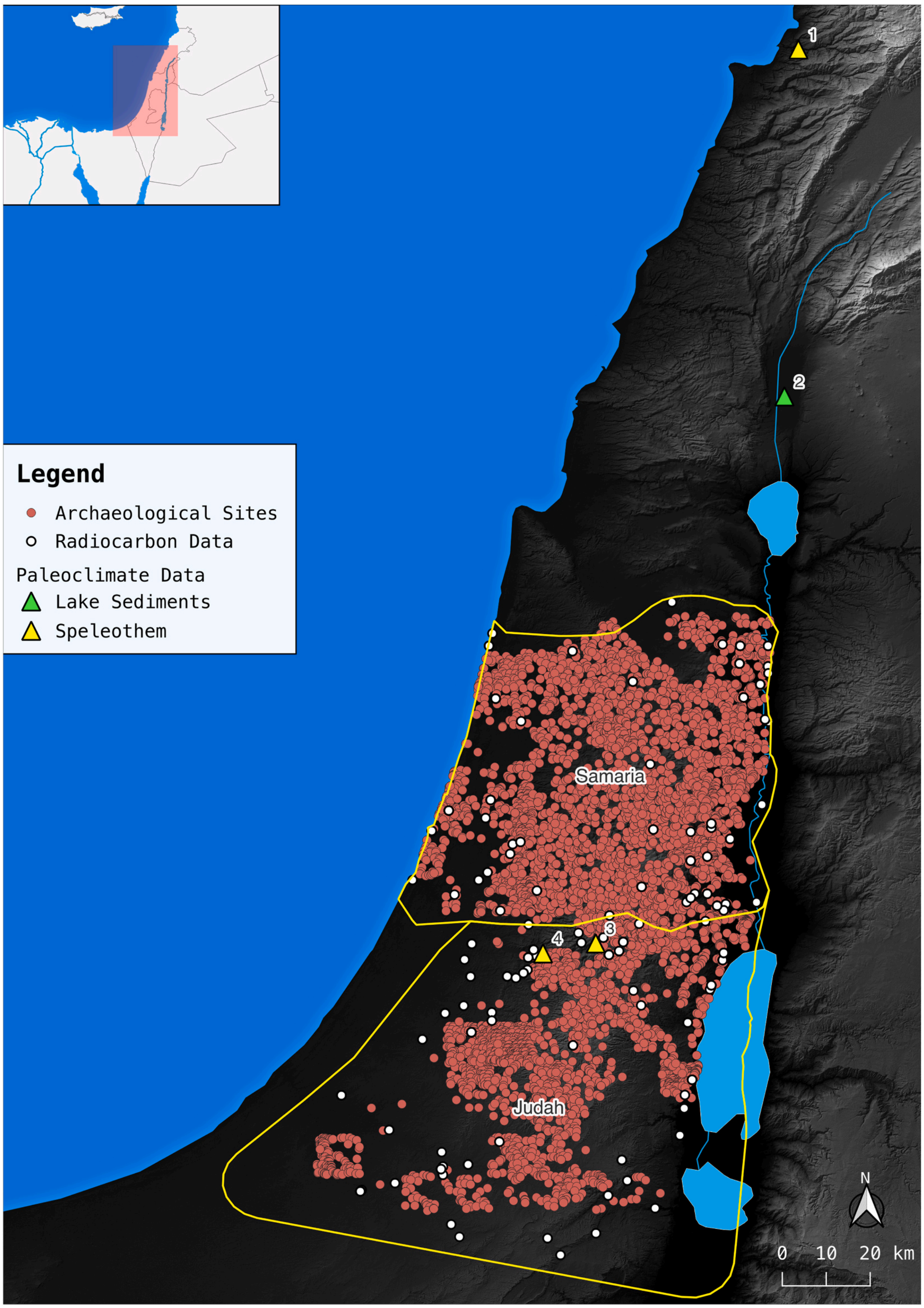


**Fig. 1.** Spatial distribution of all the dataset gathered for the project.

2021b; Roberts et al. 2011; Robles et al. 2022; Rosenzweig and Marston 2018; Sinha et al. 2019; Weiberg et al. 2019; Weiss 2016). In particular, a growing literature emphasize how the relationship between climate and population, when not framed within a deterministic point of view, can be understood as being cyclical, with periods of positive and negative correlations between the two, often viewed through the lens of population resilience rather than collapse (Allcock 2017; Bunbury et al. 2023; Cumming and Peterson 2017; Flohr et al. 2016; Greenberg 2017; Roberts et al. 2018; Roberts 2021; Weiberg and Finné 2018; Zimmermann 2012). For example, Roberts (2021) highlighted how societal reactions to climate change can be summarised as a Standard Relationship, where climate is highly correlated with population dynamics (better climate = larger population), and Inverted Relationship, where worsening climate conditions do not necessarily result in population decline (worsen climate = societal adaptation and innovation). This model is especially informative for the Late Holocene, when a decoupling of climate and population is evident, and demographic fluctuations cannot be *a priori* attributed only to climate change (Langgut and Finkelstein 2023; Lawrence et al. 2016; Palmisano et al. 2021b; Roberts et al. 2019).

The South Levant represents a privileged case study for studying long-term population dynamics, given the quantity and quality of surveyed, excavated, and published data in the form of sites and radiocarbon dates. In particular, we will focus on the Cisjordan Highlands and lowlands, and a portion of the coastal plain (Fig. 1), an area roughly corresponding to the Iron Age II Assyrian province of Samaria and the semi-independent Kingdom of Judah. The choice of this area is tied to an ongoing scholarly debate regarding the archaeological, historical, and demographic trajectories of the two regions during the Iron Age and the role of the Assyrian Empire in the South Levant. In fact, this area has often been interpreted by a strand of archaeology with a biblical theoretical framework as evidence of the negative portrayal of the Assyrian empire in the Hebrew Bible, suggesting that the southern Levantine provinces, and especially *Samerina*/Samaria, fell into a state of desolation, underpopulation, and underdevelopment, while the client states (and especially Judah) thrived *despite* the presence of the Assyrians nearby (on the topic, recently Faust 2021; Palmisano and Squitieri 2023; Squitieri 2024).

In this paper, we aim to investigate the following research questions (RQs).

**RQ 1**. What are the long-term demographic trends of the two sub-regions of Samaria and Judah and how they are related to climatic fluctuations?

**RQ 2**. Is the sub-regional lens useful to highlight meaningful differences from past broader-scale analyses?

**RQ 3**. How can a long-term approach contribute to the ongoing debate on the Iron Age II historical trajectories of the two sub-regions?

We believe that the use of a long-term approach will shed light on the aforementioned Iron Age dynamics and provide a solid base for future discussions on the topic. We will tackle these questions using a multi-proxy approach for archaeological, radiocarbon, and paleoclimate data through statistical and quantitative analyses in the form of probabilistic approaches, entailing SPDs generation, aoristic techniques, and Monte Carlo simulations (see *paragraph 2.4*). All of the above will be coupled with an openly available and highly detailed dataset constructed to be as comprehensive as possible for these types of analysis (Titolo and Palmisano 2025) (and see *paragraph 2.2*).

All analyses and figures of this work are reproducible thanks to the dissemination of the datasets and scripts written in R statistical computing language (see Appendix A).

## 2. Study area, data and methods

### *2.1. Study area*

Our study area covers around 14,711 sq. km, extending within the boundaries of present-day Palestine and Israel (see Fig. 1). The location and extent of the study area were defined by a combination of factors, including the very high intensity of both archaeological data coming from field surveys and excavations and radiocarbon samples, and the need to efficiently address the question of long-term population dynamics. Our project divided this area into two sub-regions, reflecting the Iron Age II Assyrian province of Samaria and the Kingdom of Judah, based on recent historical reconstructions (Liverani 2003; Radner 2006). A small buffer of ~15 km was also employed to account for shifting boundaries and uncertainties inherent in these types of reconstructions. While the area corresponds geographically to most of the Cisjordan, we will refer in this paper to the northern and southern parts of it as "Samaria" and "Judah" respectively, to facilitate comparisons with the current debate on the area mentioned above, even though the biblical names are not appropriate for much of the period outside of the Iron Age II proper.

Generally speaking, the whole area covers a varied landscape stretching from the Jordan River valley to the East to the Mediterranean Sea to the West, and encompassing the limestone hills of the Cisjordan highlands, the coastal plain, and the northernmost section of the Negev desert (Suriano 2013). The region is generally characterised by dry summers and rainy winters (Litt et al. 2012), with local differences in geographical sub-regions, ranging from a Mediterranean zone encompassing most of the study area, with >400 mm of mean annual rainfall, to a steppe zone with a 200–300 mm mean annual rainfall, and a minimum of 100 mm along the Dead Sea (Langgut et al. 2015; Ziv et al. 2006).

The two sub-areas share some similar characteristics, especially their central, highland-based landscape. The northern sub-area encompasses the south-eastern part of the Jezreel Valley, and the two plateaus composing the central highlands until Tell en-Nasbeh and El Jib. To the west, the highlands slopes to the Northern Coastal Plain, characterised by a series of east-west wadis cutting into clay soils and sandstone ridges (*kurkar*), while to the East the highlands give space to the Jordan valley (Singer 2007; Suriano 2013). Our southern sub-area extends from the southern part on the highlands, just north of Jerusalem and up until the Arad valley. The highlands in the east drops sharply in elevation and experience low precipitation, resulting in an arid steppe. On the west, the area is instead characterised by a series of east-west valleys, plateaus and lowland hills, composed of fine-grained alluvial sediments, opening then to the south to the steppe and semi-desert regions around the Beersheva valley (Langgut et al. 2015; Singer 2007; Suriano 2013).

### *2.2. Archaeodemographic proxies*

Archaeological data in the form of settlement data have been gathered from online databases (e.g. the Archaeological survey of Israel, available at: https://survey.antiquities.org.il/index_eng.html#/, the West Bank Archaeological Database Greenberg and Keinan 2009; Keinan-Schoonbaert 2016, Keinan-Schoonbaert, 2018) and published survey reports (Bar and Zertal 2021; Bar and Zertal, 2022; Finkelstein et al. 1997; Zertal 2004; *2007*; Zertal and Bar 2017; Zertal and Bar, 2019; Zertal and Mirkam 2016). These data were then harmonised and refined with more recent excavation data, intensive site-based surveys, and regional demographic studies (e.g. Broshi 1979; Broshi and Finkelstein 1992; Broshi and Gophna 1984; Broshi and Gophna, 1986; Fantalkin and Tal 2009; Faust 2013; Finkelstein 2011; Finkelstein, 2018; Finkelstein and Gophna 1993; Gophna and Paz 2014; Gophna and Portugali 1988; Utziel and Shai 2010) to enhance the original dataset and to avoid misinterpretations due to partial use of data.

In order to properly evaluate population dynamics, only sites with evidence of habitation were gathered in the database, thus excluding industrial sites (mines, quarries, etc.), cemeteries, or isolated land management features. Each period of occupation of a site was registered as a site-phase, corresponding to a distinct geometry in the geodatabase (Palmisano et al. 2017), and recorded with an estimated start and end date. A level of harmonisation was applied to the different source materials in order to maximise comparative potential across different surveys (Greenberg and Keinan 2009; Mazar 2011; Sharon 2013) (See also Table 1 for the chronological scheme adopted). Site extent was also directly recorded when available or calculated or interpolated when possible, and the resulting data amount to a total of 3153 archaeological sites, and 6331 site-phases for the period between 6500 and 2200 BP (the whole database contains 5542 archaeological sites, and 14,142 site-phases). The archaeological database is freely accessible online via Zenodo (https://doi.org/10.5281/zenodo.15111732), and the reader is referred to the corresponding data paper for more details on the dataset itself and its creation (Titolo and Palmisano 2025).

A total of 1378 radiocarbon dates were also collected from the open and freely available NERD dataset (Palmisano et al. 2022b), and refined with missing dates from the XRONOS database (Roe et al. 2025; Roe and Hinz 2022). The amount of available radiocarbon dates is still well within the recommended minimum threshold of 200–500 dates to produce a reliable SPD over a time interval of 10,000 years (Timpson et al. 2014; Williams 2012). All the radiocarbon dates collected come from archaeological contexts, with the majority being samples of charcoal, seeds, grain, and bone. Radiocarbon dates from marine samples, such as shells were removed in order to avoid issues arising from marine reservoir offsets (Palmisano et al. 2019).

While great care has been taken into gathering and harmonising the whole archaeological evidence available without falling into over-sampling, archaeological survey results are inevitably patchy (Bevan et al. 2013; Cassis et al. 2018; Cherry 1983) due to taphonomic loss, modern activities, sampling strategy and intensity, project/institutions interests and goals, available funding, etc. (Attema et al. 2020; Cassis et al. 2018; Rayne et al. 2020; Wilkinson 2000, Wilkinson, 2003). This is especially evident in the spatial distribution of the available data, with clear "hotspots" in the central and northern parts of the study area, and with fewer data for the southern regions (with the exception of the area around Lachish) (Fig. 2 and Table 2). Similar limitations also apply for radiocarbon dating. In fact, it is well-known that, for especially for the Late Iron Age and subsequent periods, artificial drops in demographic curves are generated from the relatively lower number of radiocarbon dates available. This is because instead of collecting and using radiocarbon samples, researchers tended to rely on chrono-typological schemes defined by pottery types and coins for dating archaeological layers, an issue further exacerbated by the presence of the so-called "Hallstat Plataeu" (a flattening in the calibration curve between 2750 and 2350 BP, Van der Plicht, 2004), that discouraged the collection of radiocarbon samples for this period (Bevan and Crema 2020; Crema 2022; Palmisano et al. 2021a; Palmisano 2023).

**Table 1**
*Chronological table for the Levant (after Mazar, 2011; Palmisano et al., 2019; Sharon, 2013).*

| Name | Dates (BCE-CE) | Dates (BP) |
|---|---|---|
| Chalcolithic | 4500–3800 BCE | 6450-5750 BP |
| Early Bronze Age IA | 3800-3300 BCE | 5750-5250 BP |
| Early Bronze Age IB | 3300-3050 BCE | 5250-5000 BP |
| Early Bronze Age II | 3050-2850 BCE | 5000-4800 BP |
| Early Bronze Age III | 2850-2500 BCE | 4800-4450 BP |
| Intermediate Bronze Age/Early Bronze Age IV | 2500-2000 BCE | 4450-3950 BP |
| Middle Bronze *Age*I | 2000-1750 BCE | 3950-3700 BP |
| Middle Bronze Age II-III | 1750-1550 BCE | 3700-3500 BP |
| Late Bronze *Age*I | 1550-1400 BCE | 3500-3350 BP |
| Late Bronze Age II | 1400-1200 BCE | 3350-3150 BP |
| Late Bronze Age III | 1200-1150 BCE | 3150-3100 BP |
| Iron *Age*I | 1150-980 BCE | 3100-2930 BP |
| Iron Age IIA | 980-830 BCE | 2930-2780 BP |
| Iron Age IIB | 830-720 BCE | 2780-2670 BP |
| Iron Age IIC | 720-539 BCE | 2670-2489 BP |
| Iron Age III (Persian) | 539-333 BCE | 2489-2283 BP |

### 2.3. Paleoclimatic records

In this paper, we used paleoclimatic proxies representing past hydroclimatic patterns, while excluding temperature-related records – since they are not necessarily linked to water availability – and pollen-based climate reconstructions, as these respond only indirectly to climate and are shaped by additional factors such as vegetation dynamics and human activity. We also selected published datasets that were freely available online. For this type of analysis, raw data in the form of stable oxygen isotope ratios ($\delta^{18}O$) from cave speleothems (stalagmites calcite) and lake sediments are usually employed to infer past hydroclimate. Due to their sensitivity to meteorological changes (e.g. rainfall intensity) that affect runoff and groundwater recharge generation, changes in isotope ratios are often interpreted as reflecting fluctuations in the amount of precipitation (Bar-Matthews et al. 2003; Cheng et al. 2015; Fleitmann et al. 2007; Flohr et al. 2017; Jones et al. 2019). The generally accepted interpretation of isotope values maintains that higher values indicate drier conditions, while lower values indicate wetter conditions. However, this interpretation is not straightforward, as each context can be highly affected by local environmental factors, such as vegetation cover, recharge conditions, open water evaporation, in-cave processes, or general geographical location (Finné et al. 2019; Jones et al. 2019; Palmisano et al. 2021b; Roberts et al. 2008).

Our paleoclimatic dataset is composed of 4 proxies (See Fig. 1 and Table 3), collected from the NOAA online database (https://www.ncei.noaa.gov/products/paleoclimatology). We collected records closer to our study area, and that could provide sufficient coverage for our time frame of analysis. Each proxy presents a different temporal resolution, and only one record (Jeita Cave) has a fine-grained resolution (<10 years), while the others vary (see Table 2 below).

### 2.4. Data processing

The use of probabilistic approaches mitigates the inherent data limitations and chronological uncertainties of archaeological data (Crema and Kobayashi 2020; Palmisano et al. 2017; Palmisano 2023; Roberts 2021).

One of these approaches employs the aoristic technique, which assumes that the probability of an event is one - meaning absolute certainty – for the occupation of a site within a specific period (Bevan et al. 2013; Crema et al. 2010; Crema 2012; Johnson 2004; Kolář et al. 2016; Ratcliffe 2000). The chronological range of the case study is divided into time blocks (in our case, 100-year), and the probability of 1 is divided by the number of time blocks that fall within the occupational period of a site (based on the material culture evidence). This process is repeated for each site, and the probability is then summed for each time block, resulting in the so-called aoristic sum, representing the probabilistic intensity of occupation in the time-block, which can then be plotted on a time-series graph as an archaeological proxy. However, it is often evident that site durations are shorter than their assigned chronological ranges based on material culture. To reconcile broad chronological uncertainties with shorter site durations, we use Monte Carlo simulations to generate randomised start occupation dates for low-resolution sites (Crema 2012; Kolář et al. 2016; Orton et al. 2017). Therefore, we drew dates from a uniform distribution across the relevant site-phase range. Each start date is paired with a site duration randomly drawn from a normal distribution (mean = 200 years, standard deviation = 50 years), corresponding to the modal phase lengths of our observed data. Although somewhat arbitrary, this assumption provides contrast with much longer uncertainties (e.g. 1000 years). We then generated 1000 randomised curves using Monte-Carlo (MC) simulation and created a 95

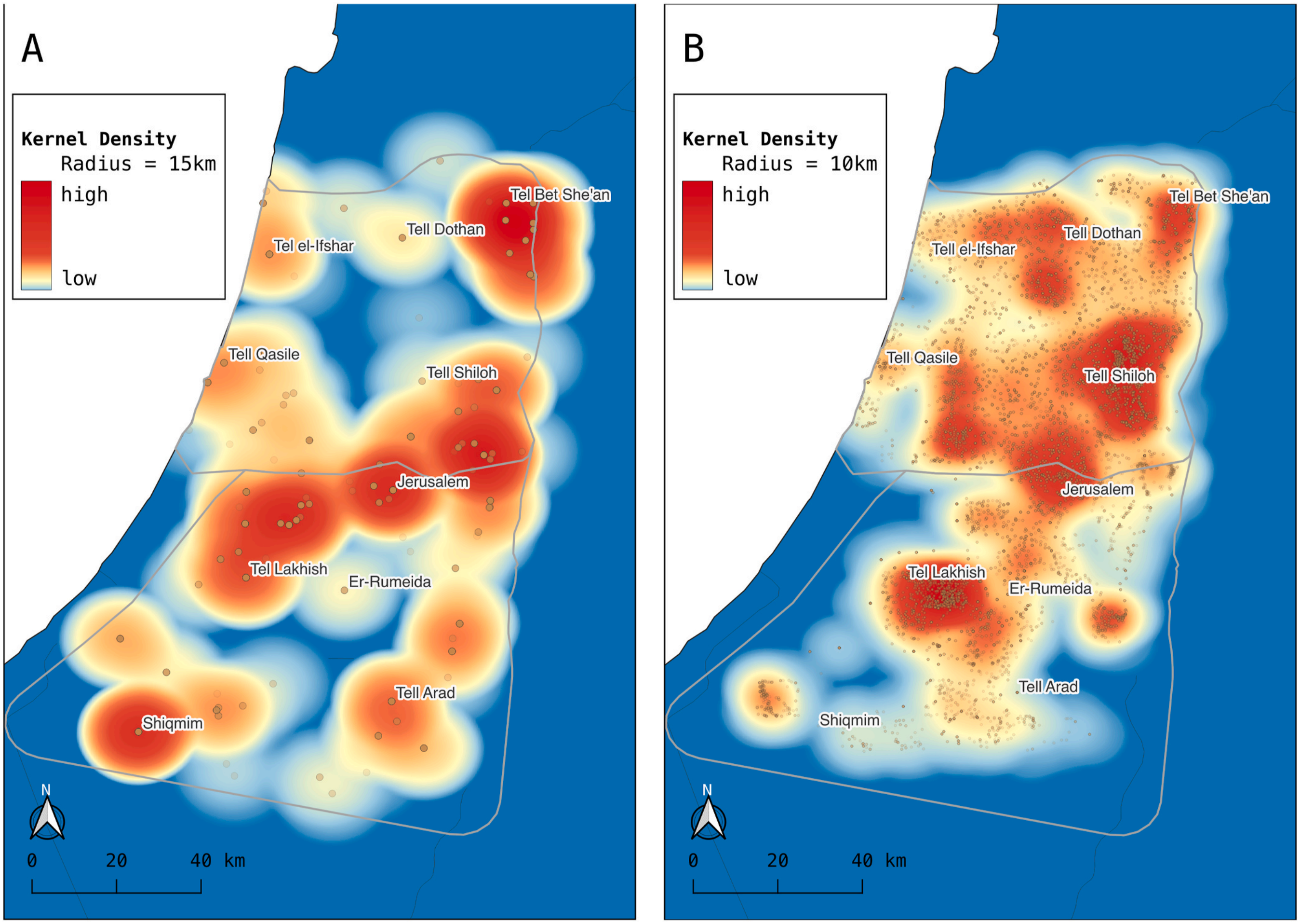


**Fig. 2.** Density of radiocarbon dates (A) and archaeological sites (B) in the study area.

**Table 2**
Archaeodemographic Proxies per sub-regions.

| No. | Name | Source | Chronological Range | Elevation (m a.s.l.) | Mean Sampling Interval (years) |
|---|---|---|---|---|---|
| 1 | Jeita Cave | Cheng et al. (2015) | 20367-372 Cal BP | 100 | 7 |
| 2 | Lake Hula | Roberts et al. (2008) | 15105-205 Cal BP | 60 | 298 |
| 3 | Soreq Cave | Bar-Matthews et al. (2003); Orland et al. (2012); Shah et al. (2013) | 30031-present | 400 | 131 |
| 4 | Jerusalem West Cave | Frumkin et al. (1999); Shah et al. (2013); | 168714-present | 700 | 550 |

**Table 3**
Paleoclimate proxies used inside the project.

| Area | N. Radiocarbon Dates | N. Sites | N. Site-phases |
|---|---|---|---|
| Samaria | 669 | 2020 | 4322 |
| Judah | 708 | 1133 | 2009 |

% confidence envelope, the width of which represents the degree of temporal uncertainty in site occupation across time (Timpson et al. 2020).

Since survey data have generally coarser temporal resolution than radiocarbon dates, with occupation periods possibly spanning millennia, the aoristic approach mitigates the likely inflated occupation span of a site (Palmisano 2023). The long-term probabilistic distribution of site frequencies based on the aoristic sum, combined with the Monte Carlo simulation, offers a useful comparison to inspect the observed patterns of raw site count data. In addition to these data, we also employed estimated site size to understand if a carefully reconstructed extent could provide another valuable proxy in demographic analyses, as already suggested by previous studies (Palmisano et al. 2017).

As for radiocarbon dates, probabilistic approaches entail generating Summed Probability Distributions of calibrated radiocarbon dates (SPD). In this process, each date is calibrated against a calibration curve (in our case IntCal20), and transformed into a probabilistic curve. Binning (in our case 100-year) is applied to mitigate spatial and temporal homogeneity derived by the aforementioned limitations (Crema 2022), and the resulting distribution for each sample is then summed to obtain a curve that represents equally each site-phase (Timpson et al. 2014, *2020*). The observed SPDs are then compared against a statistical model of growth (either logistic or exponential), generated from the observed data through a series (1000) of Monte-Carlo simulations. This test highlights meaningful departures from an expected curve produced by mere chance, and allows the observed SPD to be interpreted confidently (Crema 2022; Timpson et al. 2020). We also generated a bootstrapped composite kernel density estimation (cKDE, Crema 2022), to inspect the robustness of the curve generated through the SPD approach. The cKDE aims to smooth out noise and models not only measurement errors or calibration effects, but also the uncertainty related to sampling procedure and biases (e.g. archaeological excavation), generating a much smoother curve than the regular SPD. The cKDE is a composite process: after $^{14}$C dates calibration and binning, a calendar year is sampled from each bin, and the kernel density is estimated for the sampled ages, using a 100-year bandwidth. These steps are repeated 1000 times, to produce a 95 % confidence envelope of bootstrap cKDE (McLaughlin 2019; Palmisano et al. 2021a). If the confidence interval is narrow, it is likely that the observed pattern represents a good picture of reality.

Regarding paleoclimate data, we calculated z-scores (a standard measurement unit of variance) for each proxy in order to compare their trends and to highlight areas with similar or different climate trajectories across time (Finné et al. 2019; Labuhn et al. 2016; Roberts 2021).

## 3. Results

### 3.1. Demographic trends from SPD of radiocarbon dates

We generated normalised SPD and cKDE of 1377 calibrated radiocarbon dates for the chronological span of 6400–2200 BP with 100-year bins. Fig. 3a shows (for the whole area) that the two curves (normalised SPDs and cKDE) depict very similar trends, indicating that while biases in the sampling for radiocarbon dating are well-known especially for the Early Bronze Age and Iron Age (Braun 2012; Finkelstein and Piasetzky 2010; Finkelstein and Piasetzky, 2011; Herzog and Singer-Avitz 2006; Mazar 2011; Mazar and Ramsey 2008; Mazar and Ramsey, 2010; Nigro et al. 2019; Regev et al. 2012; Webster et al. 2023), they don't seem to have significant effects on the resulting SPDs.

The normalised SPDs are then compared to two 95 % confidence envelopes for exponential and logistic null model (Fig. 3b and c) respectively. Positive (red) and negative (blue) deviations from the null growth model indicate patterns of population growth and decline greater than expected from an exponential or logistic long-term trend. The results show non-coinciding deviations, but according to the observed p-value (0.009 and 0.001), we can generally assert that the regional population did not grow neither exponentially nor logistically in the long run. Significant positive deviations are evident for both models between 5000 and 4800 and from 3200 to 2700 BP, albeit in a lower magnitude in the comparison with the exponential model. The comparison with the logistic models also reveals additional periods of growth, for example from 6200 to 6000/5900 BP and from 5400 BP to 5300 BP, while also revealing negative deviations, from 4300 BP to 3950 BP, and then again in a shorter interval between 3700 and 3550 BP. The sudden drop around 2700 BP is likely artificial and not really reflective of past population trends, but probably related to the lower reliance on radiocarbon for dating, likely due to a combination of the effect of the so-called Hallstatt Plateau (Van der Plicht, 2004), and an increase in the accuracy of ceramic typology combined with other diagnostic material culture (e.g. coins). In summary, the trends evidenced by the SPD and the cKDE show a series of population increase starting as early as 6200 BP, with a "positive" "booms and bust" pattern alternating between steadiness and population increase, until a "negative" pattern starting from the 4300 BP, lasting until the next and most significant increase in the observed time-span, from 3200BP. The sub-regional SPD curves

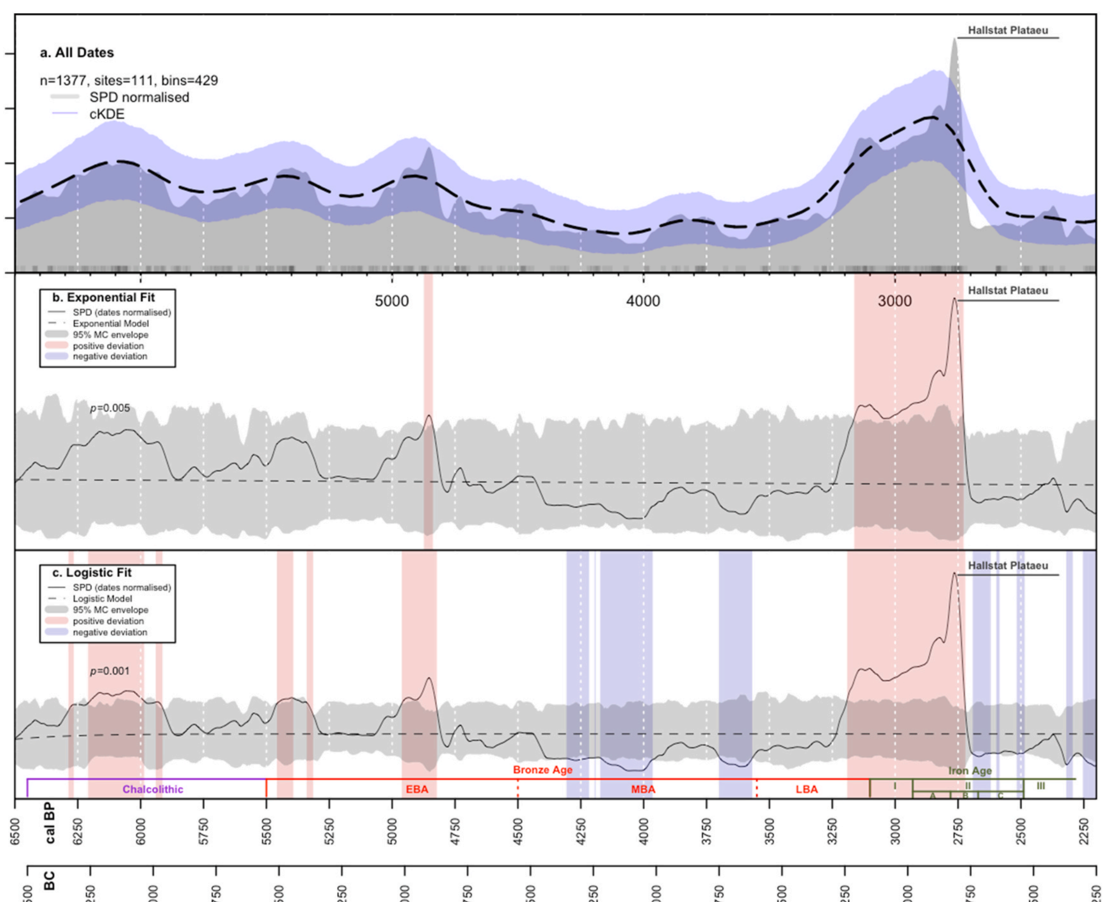


**Fig. 3.** a) Summed Probability Distribution (SPD) of normalised calibrated dates with bootstrapped composite Kernel Density Estimation (cKDE). b) Normalised dates vs. a fitted exponential model. c) Normalised dates vs. a fitted logistic model. Blue and red vertical bands indicate respectively chronological ranges within the observed SPD which deviate negatively and positively from the null model. (For interpretation of the references to colour in this figure legend, the reader is referred to the Web version of this article.)

show similar patterns and their effects on the regional curve with population increase in Samaria during 5400 and 4900 BP and a decline in 4600 and 4100 BP (Fig. 4 a) and a smaller peak in Judah around 4800 BP, with a larger decline between 4100 and 3900 BP (Fig. 4 b). Instead, the population peaks during the Iron Age between 3200 and 2700 BP in both regions.

We also investigated the differences between demographic fluctuations in the two sub-regions by employing a Permutation test (Crema et al. 2016). This is a systematic and quantitative method to analyse sub-regional divergences from the regional curve, and deal with the different sample sizes for each region. In fact, the test generates a 95 % envelope (representing the regional trend) which will be larger in regions with fewer radiocarbon dates, reflecting the uncertainty tied to having less raw data. Statistically significant deviations above or below the envelope indicate periods in which population growth or decline is greater or lower than the regional trend. As visible in Fig. 5, the two sub-regions do not show any difference in population trends when compared to the regional trends. Judah shows a negative deviation around 5000 BP, although this divergence cannot be statistically supported based on the observed p-value (0.25). Hence, we can state that the two sub-regions have almost identical demographic trends.

### 3.2. Multi-proxy results

We then compare archaeological settlements proxies (raw count of archaeological sites, total aggregated size, aoristic weight, randomised curve) with the SPD of radiocarbon dates. All proxies have been normalised on a scale from 0 to 1 in order to make the comparison possible and easier to interpret (owing also to the fact that all proxies had been binned into the same 100-year time slices).

Despite the different chronological resolution of the radiocarbon dates and the site proxies, the overall demographic trends appear roughly similar, with some points of convergence and divergence that can be highlighted (see also Table 4, Table 5, Table 6). In Tables 4–6, the Pearson correlations have been calculated up to 2800 BP, since the SPDs are not reliable beyond this point, depicting a substantial population decline that is due to some research biases discussed above. Looking at the general regional curve (Fig. 6 a), all proxies suggest a first population boom during the Chalcolithic period at around 6500 BP (4550 BC), with peaks at 6400 BP to 5900 BP. During the Early Bronze Age, the radiocarbon data point at a rise in population split in two different cycles between EBA IA (5500 BP), followed by a drop at the beginning of EBA IB (5300 BP) and a new rise at the end of EBA II/beginning of EBA III (4900 BP), while the archaeological proxies points to a population stagnation, likely due to a combination of lower resolution survey data and the mixing of the sub-regional curves, as seen below. The downward trend after 4800 BP seems to be evident in all proxies, although the archaeological data points to an earlier decline already during the end of the EB II (~4900 BP). Similar discrepancies between SPD and archaeological proxies have already been highlighted for the larger area of the South Levant as a whole in previous studies (Palmisano et al. 2019, 2021b), and attributed to a research bias, specifically to a focus of archaeologists to sample more radiocarbon dates for earlier stages of the EBA, resulting in inflated population trends. The downward trend after

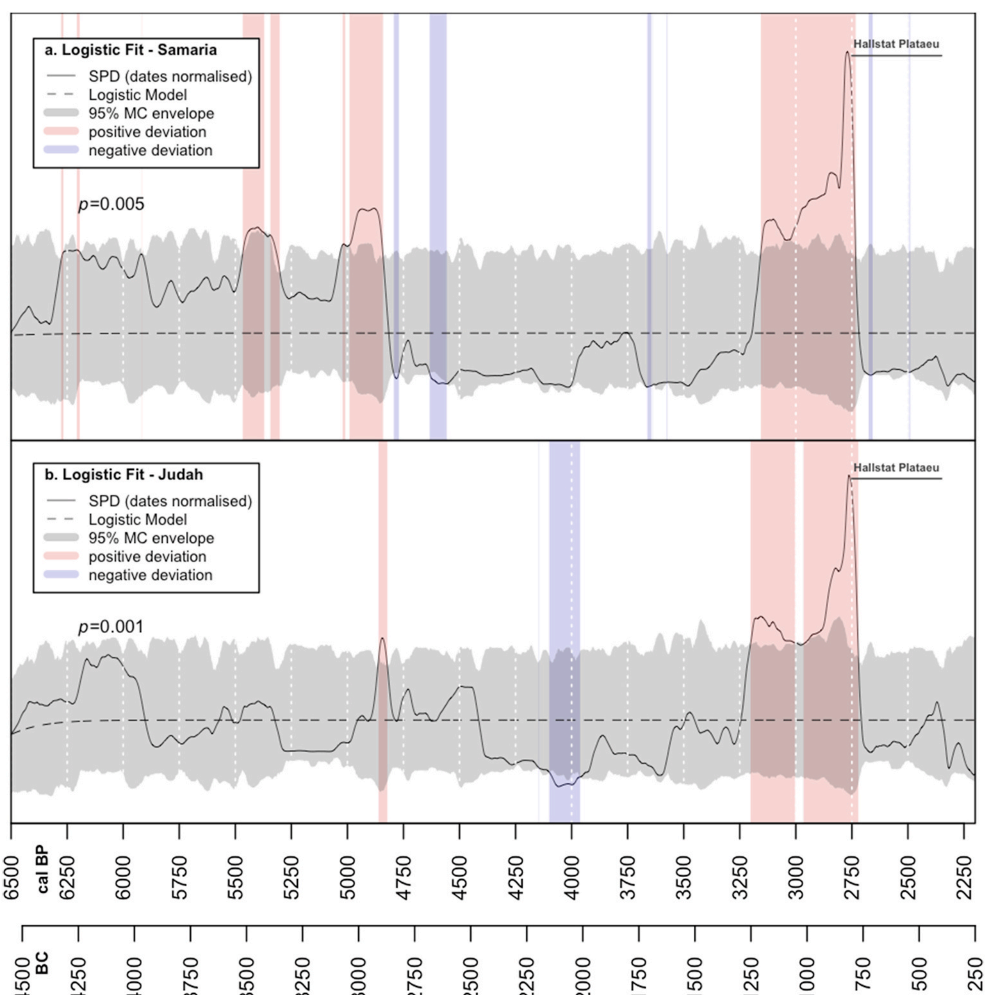


**Fig. 4.** Summed Probability Distribution (SPD) of normalised calibrated dates vs. a fitted logistic model for a) Samaria; b) Judah.

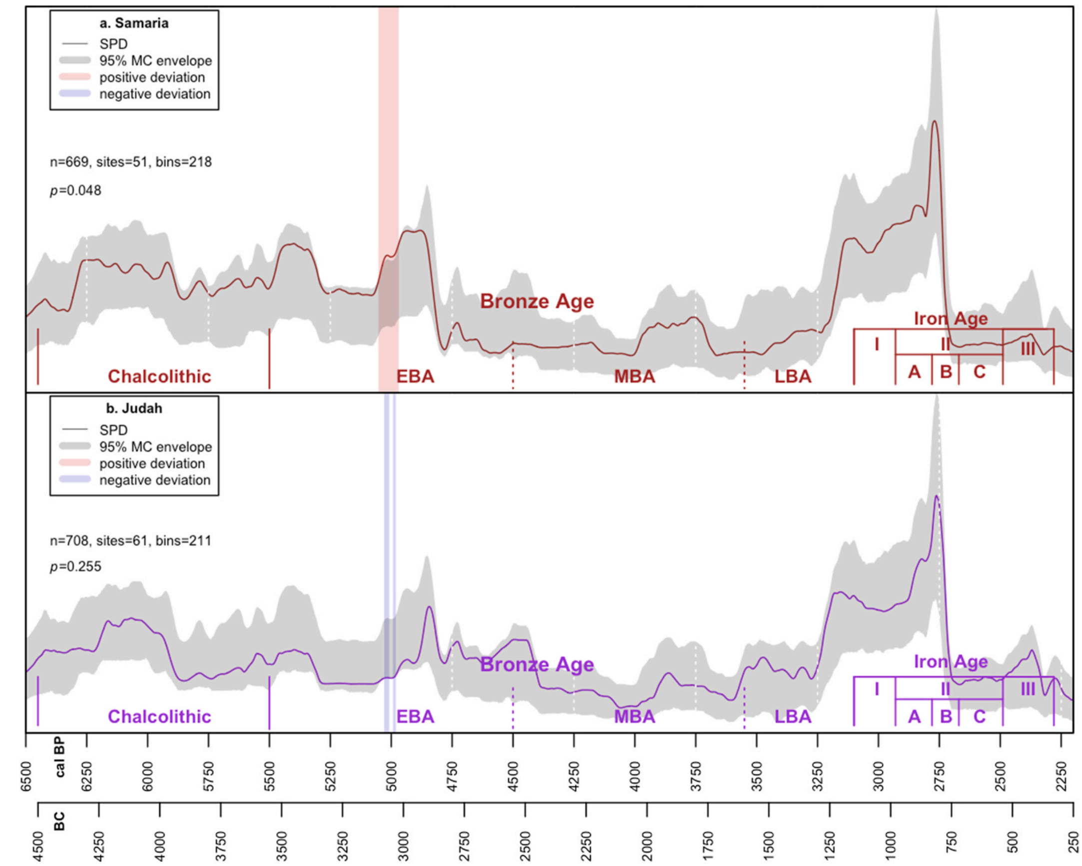


**Fig. 5.** Regional summed probability distributions (SPDs) of calibrated radiocarbon dates for a Samaria and b Judah, compared with a 95 % Monte Carlo envelope of the supra-regional model produced via permutation of regional dates.

**Table 4**
Pearson's correlation of archaeodemographic proxies between 6450 BP to 2800 BP.

| | Count | Area | Aoristic Weight | MC Simulated | SPDs |
|---|---|---|---|---|---|
| Count | 1 | 0.98 | 0.89 | 0.9 | 0.61 |
| Area | 0.98 | 1 | 0.87 | 0.87 | 0.63 |
| Aoristc Weight | 0.89 | 0.87 | 1 | 0.97 | 0.52 |
| Simulated | 0.9 | 0.87 | 0.97 | 1 | 0.51 |
| SPDs | 0.61 | 0.63 | 0.52 | 0.51 | 1 |

**Table 5**
Pearson's correlation of archaeodemographic proxies for Samaria between 6450 BP to 2800 BP.

| | Count | Aoristic Weight | Area | MC Simulated | SPD |
|---|---|---|---|---|---|
| Count | 1 | 0.92 | 0.96 | 0.93 | 0.51 |
| Aoristic Weight | 0.92 | 1 | 0.85 | 0.97 | 0.38 |
| Area | 0.96 | 0.85 | 1 | 0.86 | 0.58 |
| Simulated | 0.93 | 0.97 | 0.86 | 1 | 0.36 |
| SPD | 0.51 | 0.38 | 0.58 | 0.36 | 1 |

4800 BP seems to reverse during the Middle Bronze Age (3950-3500 BP), with all the proxies pointing towards a rise in population. However, the proxies disagree on the peak of this increase, with the radiocarbon data pointing at the MBA I (3800 BP), while archaeological data pointing to MBA II-III (3700-3500 BP), a discrepancy likely a result of the lower number of radiocarbon dates for the later period compared to the former. All proxies do show, however, a drop in population during the end of the MBA and the Late Bronze Age, with a new rise around the beginning of the Iron Age (3200 BP). A new peak is reached during Iron Age IIB (2750 BP), immediately after which all proxies show a decline, much gentler and “stepped” in the archaeological proxies than in the radiocarbon data. The drop in radiocarbon was addressed before, while the archaeological data show a more nuanced trend, with a series of downward steps at around 2500 BP and 2300 BP.

**Table 6**
Pearson's correlation of archaeodemographic proxies for Judah between 6450 BP to 2800 BP.

| | Count | Aoristic Weight | Area | MC Simulated | SPD |
|---|---|---|---|---|---|
| Count | 1 | 0.86 | 0.95 | 0.86 | 0.58 |
| Aoristic Weight | 0.86 | 1 | 0.88 | 0.96 | 0.61 |
| Area | 0.95 | 0.88 | 1 | 0.88 | 0.64 |
| Simulated | 0.86 | 0.96 | 0.88 | 1 | 0.57 |
| SPD | 0.58 | 0.61 | 0.64 | 0.57 | 1 |

The two sub-regional curves offer the opportunity to observe a more nuanced trend. For Samaria (Fig. 6 b), the proxies are quite similar to the regional curve, with population booms during Chalcolithic and Early Bronze Age, a decline in population during the EB II-III and a stagnation during the Intermidiate Bronze Age (4450-3950 BP), a gradual increase in MBA I and a peak in MBA II (this time more in line with the radiocabon data), and finally another peak during Iron Age IIB (~2750 BP). After this peak, the population slightly declined in Iron Age IIC, with a more marked decline during the Persian period between 2500 and 2300 BP, leading to a new rise at the beginning of the Hellenistic period (2250 BP). The similarity with the regional curve is likely due to Samaria making up 2/3 of the overall sites and site-phases. For Judah (Fig. 6 c), instead, the site proxies seem to follow more closely the radiocarbon data, evidenced also by the higher Pearson's correlation between the two proxies (see Tables 5 and 6). A series of cycles is evident from a peak

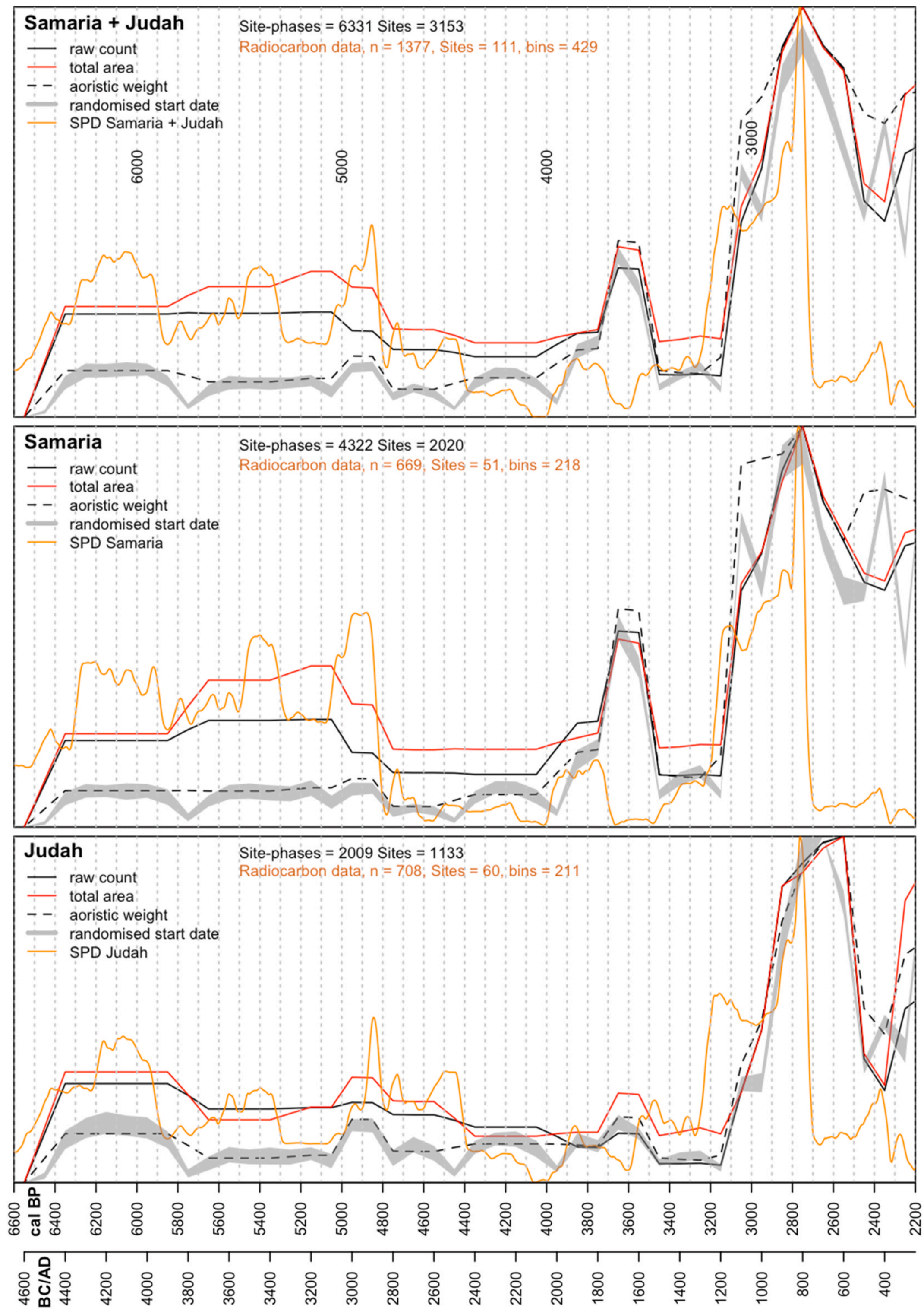


**Fig. 6.** Comparison of all archaeological proxies: sites raw count (solid line), summed estimated settlement size (red line), aoristic sum (dashed line), randomised duration of sites with uniform probability (grey envelope), and SPD of radiocarbon dates (orange line) from 6.6 ka cal. yr BP to 2.2 ka cal. yr BP. All values have been normalised between 0 and 1. (For interpretation of the references to colour in this figure legend, the reader is referred to the Web version of this article.)

during the Chalcolithic period at 6400 BP, a decline during EBA I at 5800 BP and a new smaller peak during EB II at 4900 BP. A slow population dwindling is evidenced from this point up until a new growth in population around the Middle Bronze Age II, although quickly followed by a new decline and stagnation during the Late Bronze Age. The Iron Age pattern is similar to Samaria, although the growth is more gradual and the peak is reached slightly later, in Iron Age IIC, around 2600 BP. After this, a much more significant drop in population is evidenced than in Samaria, with a smaller recovery at the beginning of the Hellenistic period.

In summary, the fact that the archaeo-demographic proxies generally agree on most parts of the investigated time-frame highlights the reliability of SPDs for inferring past demographic trends, but also the importance of integrating other proxies (e.g. sites) to contextualise and complement the SPDs results. This is especially important because we already mentioned the research bias in radiocarbon sampling for the EBA and IA, while other periods, like the MBA, received less attention. This creates skewed results that need to be addressed by cross-comparing multiple datasets (Crema 2022). While the IA site data seems to corroborate the SPDs' results, for the Chalcolithic and EBA the chronological length of these periods as produced by pottery chrono-typological dating prevents a more fine-grained analysis. A decline in population is evident during the last stages of the Iron Age in all proxies; however, the difference between SPDs and archaeological data is likely to be attributed to the previously mentioned Hallstatt plateau and should be evaluated with care.

### 3.3. Combining paleoclimate data and demographic proxies

The calculation of the z-scores for each paleoclimate proxies allowed us to inspect the effect that climate events might had on long-term population trends, especially in relation to rapid climate change events (RCC, 5.2, 4.2, 3.2 k cal. yr BP, Bini et al. 2019; Hazell et al. 2022; Jones et al. 2019). Generally speaking, the climate curves show a progressive trend towards aridity during Holocene (Fig. 7). In the study area, population peaked during the Early Bronze Age IA, despite climate data suggesting a drying pattern as indicated by the Soreq Cave records, with opposite and alternating trends recorded in the Jeita Cave (Hazell et al. 2022). However, a population decline, though not statistically significant, occurs during the 5.2 k event. The population then shows a decline trend from the end of the EBA, with significant declines during the MBA and LBA from 4300 to 3250 BP, coinciding with an increased aridity (although alternated with short-term episodes of dry-wet alternation). A population boom is then evident in the Iron Age after 3200 BP, with climate data suggesting increased aridity (except for the beginning of the period, as evidenced by the Jeita and Soreq cave proxies). Pearson's correlation between SPDs and Paleoclimate data for the whole period under examination shows generally positively correlated coefficients for Lake Hula and Soreq Cave, both in the general SPD curves and sub-regional curves, while correlation with Jeita Cave is almost 0 in most cases (Table 7). However, the p-value of these broader correlations is always larger than 0.05, so we cannot consider them

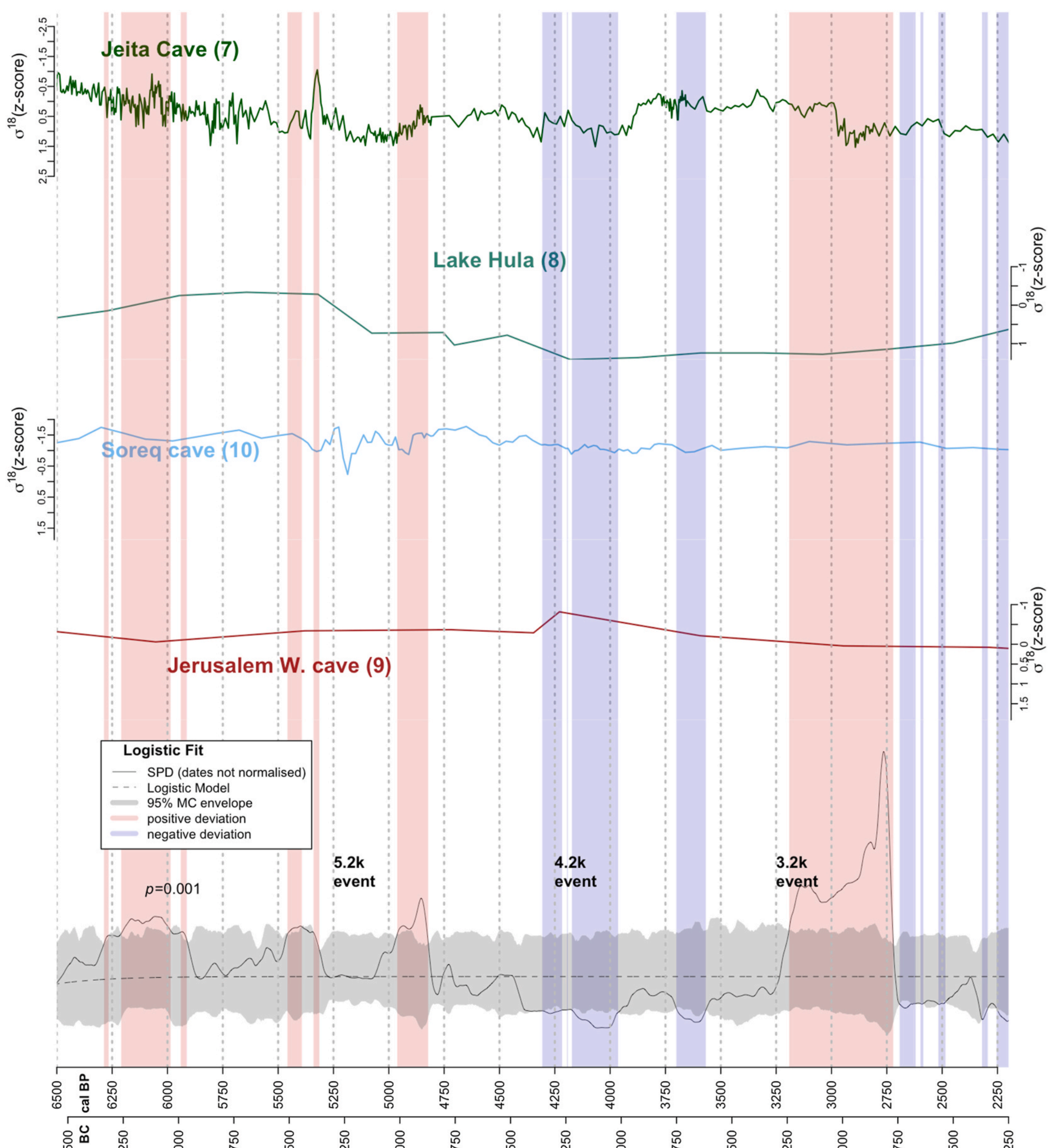


**Fig. 7.** SPD of unnormalised calibrated radiocarbon dates for the study area vs. a logistic null model (95 % confidence grey envelope) compared with palaeoclimate records from nearby sites. Blue and red vertical bands indicate respectively chronological ranges within the observed SPD which deviate negatively and positively from the null model. (For interpretation of the references to colour in this figure legend, the reader is referred to the Web version of this article.)

**Table 7**
Pearson correlation coefficients between paleoclimate z-scores and radiocarbon SPD by region between 6450 and 2200 BP.

| Region | Jeita Cave | Lake Hula | Soreq Cave |
|---|---|---|---|
| All SPD | 0.052 | 0.298 | 0.419 |
| Samaria | −0.026 | 0.455 | 0.384 |
| Judah | 0.127 | 0.059 | 0.382 |

significant.

However, the results described above only provide a picture of long-term trends, with the risk of hiding short-term events and fluctuations that can dilute time-sensitive signals and result in non-significant correlations. For this reason, we adopted a moving-window approach to inspect cyclical patterns of climate-population relation (Palmisano et al. 2019, 2021b; Roberts 2021). The moving-window approach is based on analysing the relation between two time series over time by calculating correlations within sequential overlapping windows. The method has the advantage of identifying periods of convergence and divergence between paleoclimate and demographic proxies over shorter periods of time compared to the previous inspection, and to assess if shorter hydro-climatic phenomena could be positively or negatively correlated with archaeo-demographic data. The approach involves the definition of a basic time resolution at which data is aggregated for analysis (that should be chosen according to the resolution of the original paleoclimate data), the aggregation of the time-series data into bins or time-blocks corresponding to the above, and the definition of the number of time-blocks that will form the window. Put simply, the data are first aggregated into bins, the Pearson correlations between the proxies are calculated within the length of the moving window, then the window shifts forward by the defined size, and the correlation is calculated for the next time range.

Since we adopted a multi-proxy approach, we adapted the moving-window method from Roberts (2021) to calculate the correlation not only between SPDs and Paleoclimate, but also between paleoclimate and archaeological proxies. Given our relatively limited window of analysis and the low resolution of most of our datasets for the same time frame (Table 2), we only calculated the moving-window correlation for Jeita Cave. In this case, we used a 500-year moving window, using ten 50-year bins in each window over the period from 6500 to 2200 BP.

The results in Fig. 8 show alternating cycles of positive and negative correlations. In the general curve (a), a strongly positive correlation between paleoclimate and archaeo-demographic proxies during Chalcolitic period (6450 BP-5750 BP) is followed by a negative correlation between archaeological proxies during EBA (while the SPDs show a slightly positive correlation), and a new positive correlation trend during Middle Bronze Age (3950-3500 BP), after which all the proxies are negatively correlated with the climate during Iron Age, a period characterised by another boom of population. The same patterns are also followed in the sub-regional curves (Fig. 8b and c), with the only significant difference of Judah's SPDs being positively correlated with the climate at the end of the EBA between 5000 and 4800 BP.

## 4. Discussion

### 4.1. Chalcolithic (6450-5750 BP)

Between the 4500 to 3800 BC Southern Levant experienced a population boom coupled with fundamental changes in almost every aspect of society, with an increase in settlement numbers and size (Finkelstein

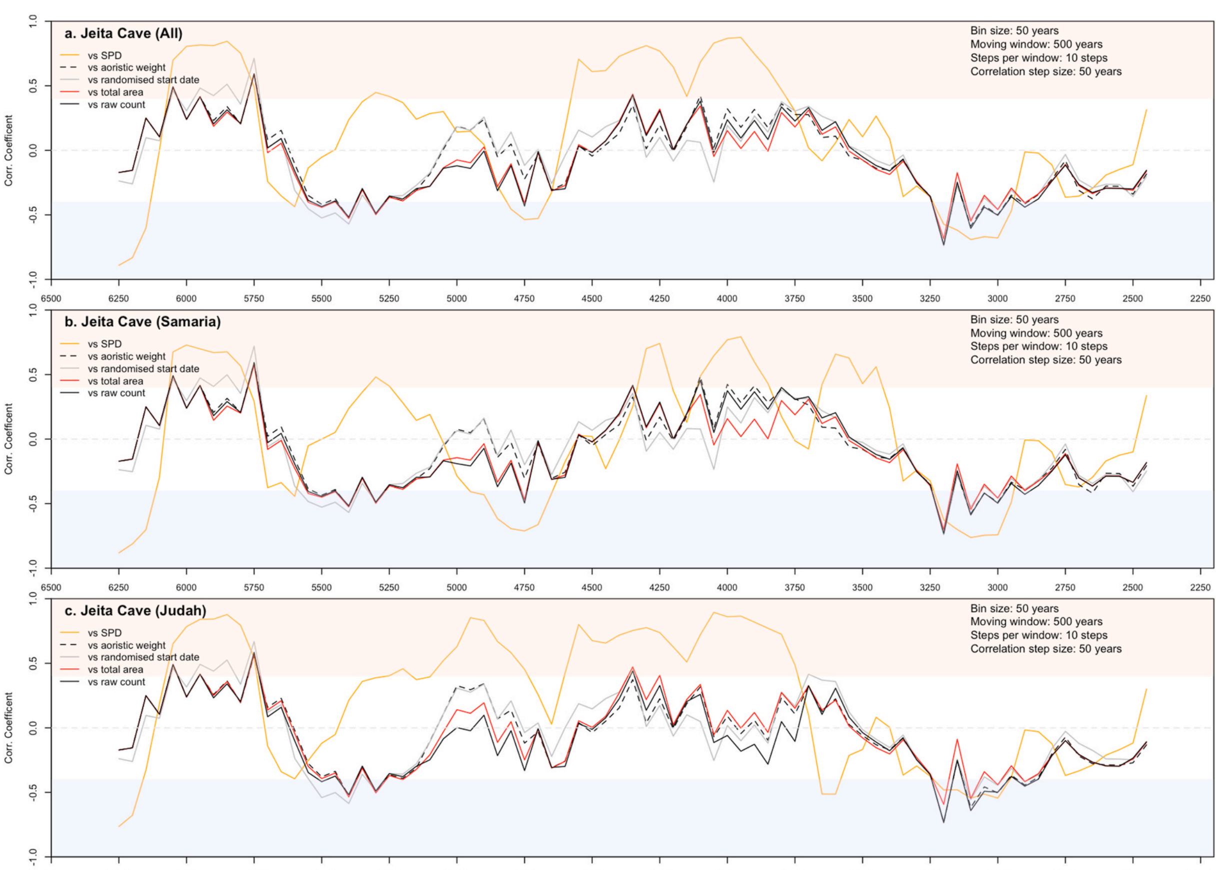


**Fig. 8.** Moving window statistical correlation plot between Jeita paleoclimate data and archaeological proxies. The orange band shows highly positive Pearson correlation area, while the blue band shows highly negative correlation area. (For interpretation of the references to colour in this figure legend, the reader is referred to the Web version of this article.)

and Gophna 1993; Levy et al. 2006), advances in metallurgical productions (Goren 2014; Levy and Shalev 1989), changes in material culture, burial traditions and subsistence economy (Rowan 2013, Rowan, 2018), albeit with a certain degree of continuity with the preceding Late Neolithic period (Banning 2007; Rowan and Golden 2009). Archaeological, paleobotanical, and faunal evidence indicate increased sedentarisation, intensification of farming strategies and diversification of crops (Besnard et al. 2013; Grigson 1998; Rowan 2013)

The above trends are well highlighted in both the regional curve and in the two study areas, with our southern study region exhibiting a larger growth compared to the northern part. Sites are generally concentrated in clusters (Mazar 2009; Rowan 2013) mainly along wadis, the Jordan valley, the central hills, and the coastal areas (Fig. 9 a); in the North they are generally small (<5–6 ha, e.g. Tell Tzaf, Fazael cluster, Tel Gezer), but larger (~10 ha) and more numerous sites are especially evident in the South, such as Shiqmim, Abu Matar, or Gilat (Gophna and Portugali 1988; Levy 1998). While the climate in the Middle Holocene was already on a path of drier conditions, records from the Soreq cave and the Lake Huka indicate more favourable conditions, especially during Late Chalcolithic (Bar-Matthews et al. 1997, 1998), while Jeita cave exhibits many sub-centennial variations between wet and dry periods. The wetter climate probably contributed to the settlement expansion in marginal zones, especially in the South of our study area, towards the Negev plateau (Rosen 1987, 2008) and to the larger expansion of the Beersheba valley settlement (Goldberg and Rosen 1987; Golden 2009), also evidenced by the positive correlation between archaeo-demographic proxies and climate (Fig. 8).

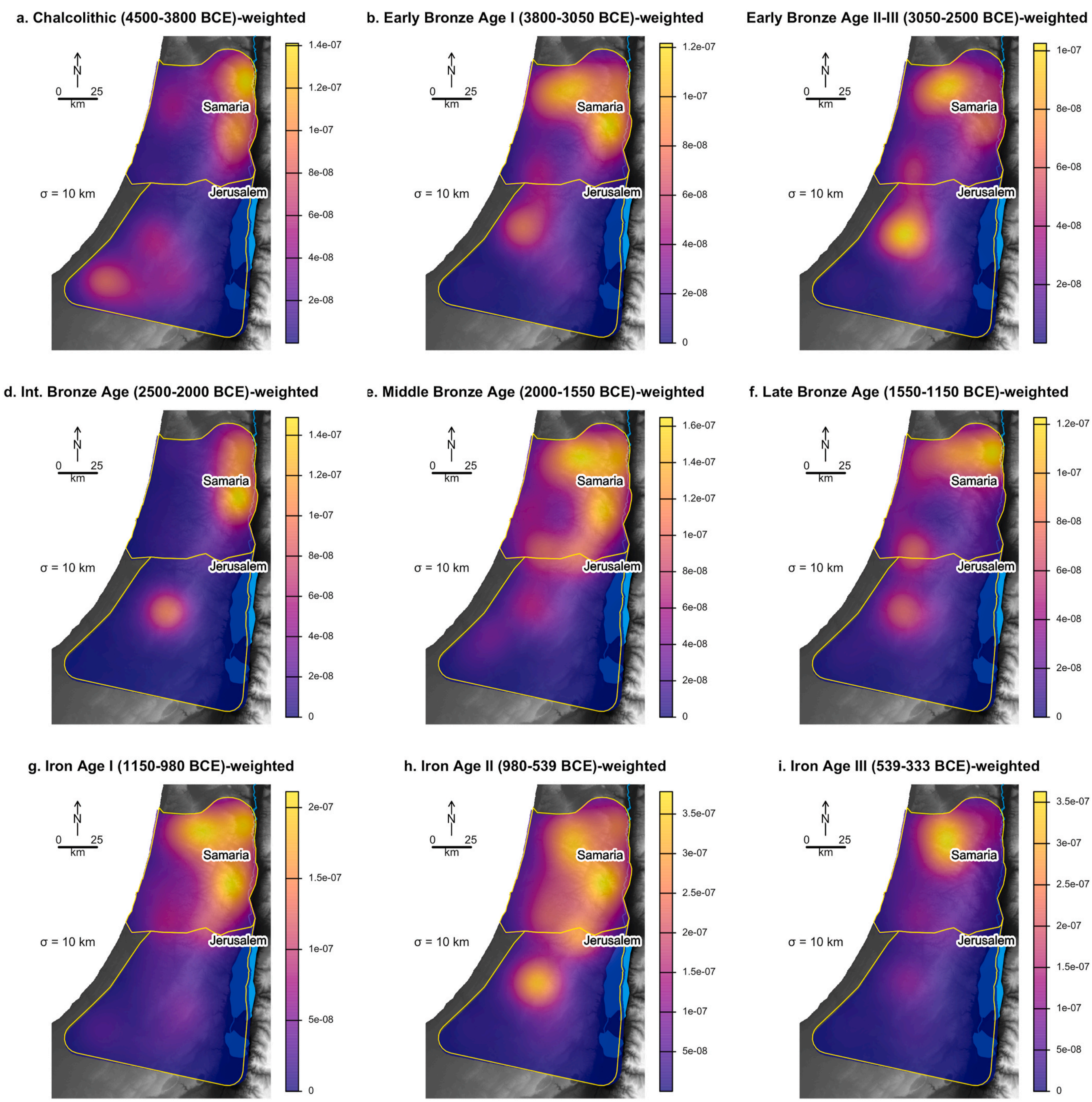


**Fig. 9.** Archaeological Settlement Density for each period under examination.

### 4.2. Bronze Age (5750-3100 BP)

Generally speaking, the Bronze Age in South Levant is characterised by patterns of population booms and busts with significant periods of population increase in EBA I-II (~5600–4700 BP) and MBA (~4000–3600 BP) are interrupted by population decline during the IBA (~4500–4000 BP) and the LBA (~3400–3150 BP) (Bar 2013; Broshi and Gophna 1984; *1986*; Bunimovitz 1998; Falconer and Savage 2009; Finkelstein and Gophna 1993; Gophna and Portugali 1988; Greenberg 2017; Savage and Falconer 2003).

#### 4.2.1. Early Bronze Age (5750-4450 BP) and Intermidiate Bronze Age (4450-3950 BP)

The Early Bronze Age in the South Levant has shown an earlier phase of population decrease and settlement restructure in EB IA, followed by a new demographic boom in EB IB (Palmisano et al. 2019). This period is often marked as a non-urban, formative stage for the urbanisation process taking place in EB II (Greenberg 2013). The population boomed in EB I-II, but settlement patterns show a decreasing trend during the transition between EB IB and EB II-III, a phenomenon interpreted as evidence of consolidation of the urban fabric of the South Levant around fewer, but larger and walled cities (Chesson 2018; Finkelstein and Gophna 1993; Gophna and Portugali 1988; Zertal 1993). The wave of new settlements in EB I and the development of urban ones in EB IB-II was accompanied by intensification of agricultural practices with the development of irrigation and water technologies, intensification of metallurgical activities and inter-regional and foreign contacts, and significant modification to the surrounding landscape (Chesson 2018; de Miroschedji 2013; Hauptmann 2003; Philip 2003). At the end of the EB III (~4500 BP), a sharp decline in settlement and population has always been suggested, usually supported by the evidence of abandonment or destruction on many EBA sites (Gophna and Portugali 1988; Mazar 2009). Recent evidence, however, suggests that rather than a complete societal collapse, the IBA (4500- 3900 BP) shows a degree of regional variations (Greenberg 2019; Palmisano et al. 2019), and should be interpreted as a more localised and regionalised society, characterised by multiple subsistence strategies adapted to the local environmental conditions of each landscape zone (Cohen 2018).

Our two areas, while mimicking the general trend highlighted above, seem to follow slightly different timings. In the northern part, demographic trends clearly indicate a series of population booms around 5500 BP and 5000 BP (Fig. 6). While this pattern might be biased due to the higher number of radiocarbon sampling in the Bronze Age (see above), settlement data also points to a (slightly more moderate) increase in number of sites at the beginning of the period (probably an issue of pottery attribution), accompanied by the settling of highland and coastal areas (Finkelstein and Gophna 1993; Gophna and Paz 2014) (see also Fig. 9 b). A decline in settlement during the EB II-III is emphasised by survey data, especially in the eastern valleys, the middle Jordan valley, and Shechem syncline (Bar 2013; Zertal 2004; *2007*; Zertal and Bar 2019) (and see Fig. 9 c). Relevant is also the significant increase in the total settled area visible in the site data in Fig. 6. This latter is probably a good proxy evidence of the population aggregation in major sites such as Khirbet et Tell, Tell el-Farah North during EB II-III (Chesson 2018; Gophna and Portugali 1988), leading to their increased size and a decline in overall raw settlement numbers. While the increased size is charted already from the EB I in Fig. 6, this is likely a byproduct of the difficulties in discerning settlement sizes over different periods and should not be interpreted as a real pattern. As mentioned above, lower resolution ceramic dating of survey data might also be the reason for the general flat curve in EB I (Finkelstein et al. 1997; Finkelstein and Gophna 1993). In Judah, the demographic and settlement data seem to decrease in the transition from Chalcolithic to EB I, and they only reach a peak during EB II (Fig. 6), with major settlements like Tell Arad or Tell Yarmuth measuring more than 10 ha. Once again we might argue that survey data do not provide fine-resolution EB I data, however, there are at least two different explanations for the observed pattern: one could be that, as mentioned by other scholars, EB I sites in the Judah area have often been erroneously attributed to Chalcolithic period (Davidovich 2012, Davidovich, 2013), so the visible pattern might not be as clear-cut as it is now. The other explanation is that in the north Negev EB I sites tend not only to be harder to identify because of the volatile nature of the nomadic element present in the area (Rosen 2008), but most importantly, an overall increase in the number of sites is mostly attributed to EB II (Finkelstein et al. 2018; Rosen 2011), while the decline after Chalcolithic might be attributed to a short dry event around 5600 BP (Clarke et al. 2016; Langgut et al. 2016). One needs to remember that this period is also the only one that the Permutation test (Fig. 5) highlights as having an actual significant difference between the two sub-regions (specifically the period around 5000 BP, i.e. the transition from EB IB to EB II), so while keeping the limitation of the data, the trend might actually be representative of a true difference between the two sub-regions. While the generally humid climate reconstructed for both EB I and EB II-III (Bar-Matthews and Ayalon 2011) (and see Fig. 7) might have facilitated the settlement expansions and the urban sites growth, the changes in settlement patterns and social organization evidenced by archaeological data, or in different agricultural practices evidenced by archaeobotanical data (e.g. the decline in olive cultivation in the transition between EB I and EB II Langgut et al., 2019) seem to be less related to climate and more affected by local and regional political and economic processes and decisions (Langgut and Finkelstein 2023), an explanation that also fit the generally negative correlation of settlement data with climate during the EBA (Fig. 8).

Radiocarbon SPDs for both areas suggest low population levels for the period between 4400 and 3900 BP; however, settlement data, while showing an overall decrease, seem to indicate a stagnation after the EB II-III decline in Samaria, and a more gradual decline in Judah. Correlation between climate proxies of the Jeita cave also shows a strong positive correlation between the SPDs, but only a weak correlation with the settlement data (Fig. 8). In Samaria, settlement patterns show a shrinking of occupation (already started in EB III), now concentrated around the north and north-eastern fringes of the sub-region (Fig. 9). The interpretation for Judah needs to be approached more cautiously: while the abandonment of Arad at the end of the EB II probably moved the region centre of gravity elsewhere, and the southern and possibly central Negev shows a new settlement wave in the IBA (Finkelstein et al. 2018), this phenomenon is way less pronounced in the Northern Negev (Rosen 2011). Moreover, most of the IBA sites in our sub-region come from a single survey (Dagan 1979), thus the evidenced pattern might vary once more data are made available. The role of the 4.2k y BP RCC to explain the observed pattern has been highly debated, with paleoclimatic evidence pointing to a largely humid period at the beginning of the IBA with a drying pattern on the transition between IBA and Middle Bronze Age (Finkelstein and Langgut 2014; Langgut et al. 2016; Langgut and Finkelstein 2023). This evidence, coupled with the weak correlation between settlement data and proxy might point to a combined effect of hyper-local climate fluctuations, changes in subsistence strategies and settlement structure peculiar to each sub-region, and most importantly, to interpret the IBA as a final stage of population decline (that started earlier), rather than a sudden collapse (Adams 2017; Greenberg 2017; Grigson 1998). Moreover, taking into account the population booms in the previous periods, and considering that population levels in IBA fall within the expected values for a logistic model of growth (Fig. 4), this period could also just represent a return to more sustainable population levels after the previous "overshoot" (Cumming and Peterson 2017; Roberts 2021),as already suggested in previous studies (Palmisano et al. 2021b), while the larger decline evidenced in Judah might be representative of the fragility of the desert fringes areas to exacerbated climate conditions (as discussed below).

#### 4.2.2. Middle Bronze Age (3950-3500 BP)

The Middle Bronze Age is usually regarded as a period of reurbanisation, with profound changes in many aspects of the South Levantine society (Ilan 1998). A rise in settlement numbers is recorded almost everywhere, with areas previously inhabited now settled (Broshi and Gophna 1986; Cohen 2013; Gophna and Portugali 1988). The beginning of the period is characterised by a slow but significant demographic rise paving the way to a larger boom in the second part of the period (MB II-III). The same trend toward intensification between MB I and MB II-III is evident in foreign trade, standardisation of pottery production, and metallurgical production (Cohen 2013; Gophna and Portugali 1988; Greenberg 2019; Mazar 2009).

The sub-regions under study seem to follow the pattern highlighted above, except for the different timings. Samaria shows an increasing trend already around 4000 BP in all the archaeodemographic proxies, reaching a peak around 3700 BP. Survey indicate an extension of the settlement over almost the entire sub-region (Fig. 9 e), although with varied regional intensities (Zertal and Bar 2017), with some sites like Jenin and Tell Ta'anach that continued to be occupied, while new important sites were founded in this period (e.g. Tell Esur) (Bar and Zertal 2021; Zertal and Mirkam 2016). Judah instead shows a decline in the settlement proxies, which is also supported by most of the archaeological data, indicating a general decrease in the number of settlements during MB I, especially in the more marginal areas (Finkelstein et al. 2018; Greenberg 2019; Rosen 2011). This phenomenon might be possibly associated with a drier period at the beginning of the millennium (Finkelstein and Langgut 2014; Langgut and Finkelstein 2023) (see also Fig. 7), with the shift of trade and political centers towards the coast (Cohen 2013; Ilan 1998) and with increased pastoral activity (Palmisano et al. 2019); however, one should also keep in mind the lower reliability of archaeological proxies for the IBA highlighted above. The climate variability is probably a component in a more complex interrelation of social, economic, and political elements, and should not be regarded as a single explanatory factor as also suggested by the generally low correlation between archaeological proxies and Jeita cave speleothems (Fig. 8) (and see also Finkelstein and Langgut 2014). However, the significant departure of the SPD curve from the logistic model at the transition between IBA and MB I (Fig. 4) aand the strong positive correlation between SPDs and climate (Fig. 8), may hint at a more significant climatic effect on population dynamics in this period.

During MB II-III (~3700-3500 BP), archaeological proxies indicate a peak in population (Fig. 6) while the declining SPDs pattern is probably explained by archaeologists' over-reliance on ceramic data or other chronological synchronism for this period, and the relatively small number of available radiocarbon dates (Palmisano et al. 2021b). Both regions show a surge in settlement numbers, highlighted in the north by the expansion of sites in the highland areas of Samaria, with the foundation or extension of sites such as Tell El Fara'ah North, Tell Balata, Tell Dothan, and Tell Shiloh, and the fortification of the Jordan valley sites like Jericho and Beth She'an (Greenberg 2019; Greenberg and Keinan 2009; Ilan 1998). In Judah, most of the sites are concentrated in the central part of the region, with the density of settlement decreasing moving southward (Fig. 9 e). While settlements such as Tell Masos and Tell Malhata existed in the Beersheba region (Finkelstein and Langgut 2014; possibly due to ameliorated climate conditions, Langgut and Finkelstein 2023) a modest growth is visible around Lachish, Gezer and Beit Mirsim, with higher settlement concentrations around Tell er-Rumeida and the still small town of Jerusalem (~6ha), which was also fortified in this period (Regev et al. 2021) and surrounded by a series of satellite sites likely for its subsistence (Greenberg 2019). Faunal remains from these sites also suggest a movement to an urban-rural economy in the larger exploitation of cattle and reduction of pig percentage compared to the IBA (Edelstein et al. 1998; Horwitz 1989).

#### 4.2.3. Late Bronze Age (3500-3100 BP)

The Late Bronze Age in the South Levant is characterised by a cultural continuity with MBA polities; however, evidence from excavation, survey, and textual data suggests a deep difference between the two periods. LBA South Levant shows a significant decrease in settlement numbers, a strong regional variation between settlement sizes and hierarchy, and a generally less integrated settlement system (Bunimovitz, 1998; Panitz-Cohen, 2013; Greenberg, 2019). The population dwindled, and occupation seems to be restricted mostly in coastal areas and major valleys, abandoning the highland areas until at least the end of the period (Finkelstein 2003).

All archaeological proxies show a substantial decrease in population in the LBA (~3500–3100 BP). Low-resolution survey data do not allow a proper understanding of settlement fluctuations (which appear stagnant during the whole LBA), but the overall appearance is that of a significant reduction in sites during the whole period. The population shrinks and concentrates in the North (Bet She'an, Tell Balata) and Jordan valleys for the Samaria area, and in the central and west regions for Judah (Fig. 9 f) (Finkelstein 1996b; Finkelstein, 1996a; Jasmine 2006). The demographic boom in this region between 3200 and 3000 BP suggested by the SPDs (Fig. 4) is likely an artifact of the oversampling from the LBA IB-II levels from Lachish (Webster et al. 2019, summing up to 65 % of all the radiocarbon samples for this period in the area) and probably should be reflective of the site surroundings (Jasmine 2006) aand should not be considered as a regional pattern, given the dearth of settlements in the whole area. The concentration of sites in specific regions might be the result of an “attraction” process mostly coming from the late 14th and 13th century and probably linked to the effect of Egyptian strategy of securing strategic routes and revenues for campaigning armies, superimposed on a background of general instability (evidenced by the frequent destruction layers recovered throughout the LBA) and preexisting economy established at the end of the LB I (Greenberg 2019). In this light, the small population “bumps” visible in the SPDs of Samaria might be explained as an effect of the localised increased population in e.g. Jezreel and Jordan valleys during this period (Bunimovitz 1998; Finkelstein 1996b).

### 4.3. Iron Age (3100-2283 BP)

The Iron Age is characterised by a decline in the Egyptian domination in South Levant and a formative period of initial fragmentation in localised polities during the Iron *Age*I (Broshi and Finkelstein 1992; Finkelstein 1998; Greenberg 2019). At the beginning of Iron Age II, regional kingdoms such as Judah and Israel formed. During the last phases of Iron Age II, these local kingdoms were included in the Assyrian sphere of interest through a series of military campaigns, bringing the northern region under the provincial system of the Empire, and leaving the south as a client state. Assyrian domination lasted for around a century (~720–640 BC), paving the way for the following external imperial domination over the region (Babylonian and Persian).

A population boom is visible around ~3100 BP in both subregions (Fig. 6), but Samaria reached a peak earlier than Judah, with also an earlier drop in archaeological proxies. but Samaria reached a peak earlier than Judah, with an earlier drop in archaeological proxies. This is a well-known aspect of IA I settlement dynamics for the area, with sites concentrating in the northern and central highlands, while expanding further to the south later in the IA II, and showing only sparse settlements in the marginal areas (Faust 2018; Finkelstein 1998; Greener et al. 2018; Ilan 2018; Rosen 2011) (Fig. 9g and h). Despite a drying phase and the so-called 3.2 ka event, population increased substantially during the Iron *Age*I and was negatively correlated with paleoclimatic trends (Figs. 7 and 8).

During Iron Age II, there is a slight difference in the timing of the population peaks in the archeodemographic trends. While the SPDs show an almost identical pattern, the archaeological proxies show a delayed peak of around 150 years for Judah (Fig. 6). Dry climatic conditions during IA II (Finkelstein and Langgut 2014; Langgut and Finkelstein 2023) did not affect demographic trends (Fig. 6), suggesting that by that time, local community were less vulnerable to climate shifts (Lawrence et al. 2016; Palmisano et al. 2019)

In general, the trend visible in Judah through the settlement data is one of gradual growth when compared to Samaria. This trend seems to be connected to the local longer-term settlement dynamics of the region, such as the later occupation of the southern highlands and northern Negev during IA IIB (Finkelstein et al. 2022; Greener et al. 2018; Thareani-Sussely 2007b), and the 7th century (IA IIC) expansion in the eastern desert and dead sea marginal areas (Faust 2008; although the timing of this expansion oscillate between beginning or late phases of the century, see Mashiach and Davidovich 2023). These expansions (and the resulting population dynamics) came probably as a result of a combination of advantageous climatic conditions (Langgut and Finkelstein 2023), political stability (Faust 2018; Liverani 2014; Sergi 2023), and proximity to the Assyrian empire and to the Assyrian-dominated Arabian trade (Finkelstein 1992; Thareani 2011; Thareani-Sussely 2007a). These elements also led to a transformation in the economy from mixed Mediterranean subsistence to high-risk/high-gain specialised and region-based (Finkelstein et al. 2022). The rapid and marked population peak observed during Iron Age IIC may have undermined the stability of the regional socio-ecological system and caused a phenomenon of "overshoot" (as in Cumming and Peterson 2017; Roberts 2021), wherein population growth outpaced the available resources, resulting in the region's exceeding its carrying capacity (Marston 2023) Hence, in a general context of a drying climate trend and socio-political instability, a pronounced population decline occurred in the later Iron Age III when likely some of the resources that allowed the overshoot also came to exhaustion.

Settlements in Samaria seem to achieve prominence earlier (~2800 BP, with the aoristic sum suggesting an even larger growth in IA I), a pattern probably linked to the formation of the regional kingdom of Israel (Killebrew 2013; Sergi 2023), but its population also dwindled earlier too (~2750 BP). The decrease in number in Iron Age IIC (~2670-2489 BP), however, might be less dramatic that what is usually suggested (Faust 2015). Here, in fact we argue that not only the decline should be interpreted in the appropriate context, but also that survey data play a significant role in this picture. Most survey reports from the central and eastern part of the region highlight a strong difficulty in distinguishing between IA IIB and IIC material in survey data alone (Bar and Zertal 2022; Finkelstein et al. 1997), considering also that most of these surveys were carried out before the recognition of the (few) diagnostic pottery types (Zertal 2003). This already suggests that this issue is likely obscuring most of the settlement data for this period, with the result of sites being attributed to a wider chronological range or assigned only to the IA IIA-B (Bar and Zertal 2021; Zertal and Bar 2019; this is also due to the strong local character of the late IA II material culture Thareani 2016; and a general tendency of attributing Iron Age material culture to the earlier phases of Iron Age II, Greenberg and Keinan 2009). Considering that data from Manasseh Hill and Southern Samaria surveys accounts for more than 60 % (1881) of our total sites for the region over the whole time-range and for 73 % of our Iron Age II sites, and that only 144 IA IIC sites were reported, we argue that we are seeing a significant pattern and that this "gap" in the current knowledge is likely masking some more nuanced IA IIC phenomena, with archaeologists themselves finding "surprising" the lack of sites in fertile areas such as the Jordan valley (Zertal and Bar 2017). On this line of thought, it is worth stressing that a good portion of single-occupation Iron Age IIc evidence (52 %) from the Archaeological Survey of Israel dataset comes from very small, but excavated sites (usually in rescue excavations). Moreover, previous studies have emphasised that during Iron Age IIC the province of Samaria underwent a process of settlement reorganisation (Squitieri 2024). Rather than seeking to occupy as much land as possible, new foundations were concentrated in specific regions and settlement types (e.g. the excavated farms between Tell Hadid and Tell Aphek, Faust, 2021) as well as with specialised forms of animal husbandry (Sapir-Hen 2017). This pattern appears consistent with supra-regional Assyrian imperial strategies (Bagg 2013; Liverani 1988; *2014*; Parker 2001; Radner 2008; Thareani 2016), and studies using a different dataset show that, demographically, the region was less severely affected than what has often been assumed (Palmisano et al. 2019). Furthermore, the permutation test on SPDs of radiocarbon dates shows no significant differences between the two sub-regions (Fig. 5). Another possible explanation of this trend is that the larger chronological range adopted for the IA IIC also encompasses the fall of the Assyrian Empire and obscures the effect of the Neo-Babylonian military campaigns in the south-west (Faust 2003). Thus, a combination of archaeological visibility and chronological limitation, coupled with structural transformations in the settlement system (as in Casana 2007) may generate signals that do not necessarily indicate actual significant changes in the underlying human population (Crema 2022). Arguably, the decline in population seen from the archaeological proxies in Fig. 6 is around 15 %, is around 15 %, which is nowhere near the "devastation" argued by a lingering biblical narrative. In addition, the statistical assessment via a permutation test of the calibrated radiocarbon dates does not show any significant difference between the demographic trends occurring in Samaria and Judah during the IA IIC (Fig. 5).

During Iron Age III, settlement data show a very low population, although a much more dramatic decline is evident in Judah than in Samaria (Faust 2007; Zertal 2004).While it is generally hard to pinpoint Neo-Babylonian and Persian activities correctly in the region, it seems that especially Persian-period settlements were concentrated in coastal regions and to the North of the study area (Fig. 9 i), with the north-eastern Samaria being a particularly flourishing zone (Zertal 2004; Zertal and Mirkam 2016), while other regions were mostly devoid of settlements (Zertal 2007; Zertal and Bar 2019). Marginal areas were also likely more impacted by drying climate conditions (Greener et al. 2018; Langgut and Lipschits 2017). However, archaeological data and (partially) SPDs point to a partial demographic recovery after 2350 BP.

### *4.4. Climate-population cycles in the South Levant*

The two sub-regional dynamics show well the complex climate-population nexus as defined by Roberts (2021). Looking primarily at Figs. 7 and 8, it is possible to understand that long-term trends highlight the "Inverted Relationship" mentioned by Roberts (2021), especially in the last 1500 years of our plots. In addition, Fig. 8 seems to depict five subharmonic (1/2) 750-year regular cycles of the multi-centennial Bond cycles (~1500-year) of the Holocene from 6250 to 2500 BP. While the first four cycles show an initial positive correlation between population and climate followed by a decline, the final cycle (3250–2500 BP) displays only a negative correlation between the two. In fact, in the long term, while the climate became progressively drier, the population not only did not decline, but on the contrary, it grew, particularly in the Iron Age. This outcome is expected as complex societies might have better ways to counteract climate shifts compared to subsistence farmers (Roberts 2021; Rosen and Rivera-Collazo 2012), especially in times where the spatial scale of societal organisation was larger (e.g. in the "Age of Empires," Altaweel and Squitieri 2018; Roberts 2021). The relationship between climate, population, and society is not straightforward, even when the inverted relationship is taken into consideration. In fact, local climatic fluctuations, sub-regional geography, and most importantly, sociopolitical structure of the study areas should always be taken into consideration (Langgut and Finkelstein 2023), with sudden and shorter climatic events sometimes proving more challenging for the local population than longer dry periods (Weiberg and Finné 2018). We have seen before that while we can generally identify cycles of demographic trends (with population peaks across the EBA, MBA, IA interrupted by stagnation and decline in IBA and LBA), hardly any of the population booms or busts can be attributed exclusively to climatic conditions. The EBA population cycle likely did not end because of climate conditions (which were mostly stable throughout EB II-III), but as a result of the socio-ecological system's "connectedness" (Marston 2023) and its lower resilience to internal and external stress (Greenberg 2019*: 130*).

Most importantly, not all the climatic events had the same effect on the local population (Table 8). For example, evidence of societal resilience is likely hinted by the minimal effect of the rapid dry event in 5200 BP (Clarke et al. 2016), which was likely mitigated, though not exclusively, by the development of new irrigation technologies during the EB IB in the South Levant (Chesson 2018). The SPD of radiocarbon dates indicates a population decline between 4200 and 4000 BP (Fig. 7), while settlement data suggest the population largely stagnated across the Intermediate Bronze Age in the Southern Levant (Fig. 6). This likely reflects reduced rainfall limiting agricultural surplus, limited marginal land due to the expansion of fortified settlements during EBA II–III (~5000–4450 BP), and land overcapacity (Wilkinson et al. 2014). In contrast, the 3.2 ka event appears to have had little to no impact on the two sub-regions, showing a decoupling between demographic and climatic trends, because more complex societies were less vulnerable to exogenous climatic stresses.

More generally, strong positive (and longer) correlations between SPDs and climate data are more visible in Judah than in Samaria (Fig. 7), due to the wider presence of "fringe zones" in this sub-region. These areas would be more vulnerable to both rapid climatic events and longer dry periods, which is why major archaeodemographic booms that involved the southernmost regions are generally tied to a combination of supra-regional dynamics (e.g. either Egyptian-sponsored trade in EB II or Assyrian-controlled trade in the IA IIC) and favourable climatic conditions. Similar climatic conditions also accompanied the cycles of settlement expansion in the highland regions of both Samaria and Judah, for example in the MBA II-III and in Iron *Age*I which also favoured intensive specialised cultivation (such as olives) beyond the production aimed at local consumption (Langgut et al. 2016, Langgut et al., 2019), but at the cost of increased anthropogenic impact on the landscape (Langgut et al. 2014). The gradual growth of Judah throughout Iron Age and its rapid population decline might well resemble the overshoot pattern mentioned in Roberts (2021) and hypothesized from other regions (Brown 2017; Shennan and Sear 2020; Tallavaara and Jørgensen 2020; Weiberg et al. 2019; although see more generally Tainter 2006), when population and resource became out of sync in generally favourable and changing socio-political conditions (Faust 2018), but within a deteriorating climate trend and larger deforestation and land use pattern (Langgut et al. 2014).

## 5. Conclusions

In this paper, we investigated the demographic trends of two South-Levantine sub-regions using a finer resolution time window (100 years) compared to previous studies, and (to our knowledge) the first large dataset combining locational accuracy, size estimates, and an analysis-ready structure in a single database. This dataset allowed us to inspect long-term trends in the two study areas in a more comprehensive, systematic, and quantitative way than has been possible until now. We analysed sub-regional patterns to move beyond the picture of the whole Levant used until now, revealing how a wealth of archaeological datasets can enable a more detailed investigation of the two study areas to highlight demographic fluctuations over the long term. Our results reinforce the importance of inspecting study areas also at the sub-regional scale in order to better understand local dynamics that might be hidden when focusing on a regional perspective. Our analysis revealed that the two sub-regions followed similar but not identical patterns, with Samaria showing long-term trends that resemble the supra-regional South Levantine ones, while Judah presents a more nuanced pattern, much more influenced by a combination of climate and sociopolitical dynamics compared to the former. While the two regions diverge slightly in their trends during the last phases of the Iron Age, we argued that this is mostly a combination of archaeological visibility, chronological shortcomings, and structural changes in settlement systems, and that the small decline visible in Samaria is nowhere near the scenario of desolation usually depicted for the area after the Assyrian conquest. Our analysis also highlighted the cyclicity of climate-population relations. While we maintain that climate cannot be used as a sole interpreter of events, it is undeniable that settlement expansion and contraction in marginal or less habitable areas have also been shaped by climatic fluctuations, with possible evidence of population overshoot in Judah during the Iron Age IIC. However, as seen in the previous sections, the relationship with climate and population should be evaluated with care, period by period, especially during the Late Holocene, when the decoupling of the latter from the former is more evident (Palmisano et al. 2021b). Future endeavours will need to complement the demographic analysis with a focus on long-term settlement patterns and systems. In fact, the demographic aspect is but one signal useful to understand past historical and archaeological dynamics, which needs to be complemented by evaluating aspects of centralisation, spatial distribution, and political integration. More insight into the areas might also come from a future application of the Adaptive Cycles models with the help of a Resilience theory framework, which has already proven to be useful when coupled with survey data (Allcock 2017), and that would certainly benefit from the wealth of data the South Levant has to offer.

**Table 8**
Impact scale of RCCs on the two sub-regions.

| Region | 5.2k | 4.2k | 3.2k |
|---|---|---|---|
| Samaria | moderate | severe | negligible |
| Judah | moderate | severe | negligible |

## Author contributions

Andrea Titolo: conceptualisation, methodology, software, formal analysis, investigation, data curation, visualization, writing – original draft.

Alessio Palmisano: conceptualisation, methodology, data curation, writing – original draft, supervision, funding acquisition, project administration.

## Declaration of competing interest

All authors declare that they have no known competing financial interests or personal relationships that could have biased or influenced the work presented in this paper.

## Aknowledgements

Fundings were provided by the Gerda Henkel Stiftung for the project "Governance Policies and Political Landscapes in the Southern Levant under the Neo-Assyrian Empire" (grant number: AZ 31/F/21, PI: Alessio Palmisano; https://www.gerda-henkel-stiftung.de/en/projects?page=192), and by the Italian Ministry of University and Research – University of Turin for the project "Strategie di governo nel Levante meridionale durante la dominazione Neo-Assira" (PI: Alessio Palmisano).

## Appendix A. Supplementary data

Supplementary data to this article can be found online at https://doi.org/10.1016/j.quascirev.2025.109777.

## Data and reproducibility

Since our project strives to adhere to Open Science practices, it is our goal to ensure reproducibility of our methods and to make our code and data available online under an open license. The dataset included here provides a collection of archaeo-demographic (radiocarbon dates and archaeological settlement data) and palaeoclimatic proxies. In addition, the digital archive related to this paper allows reproducible analyses and figures trough scripts written in R statistical computing language. The digital archive is freely available on Github (https://github.com/UnitoAssyrianGovernance/tale-of-two-regions) and Zenodo (https://doi.org/10.5281/zenodo.15111732).

## References


Adams, M.J., 2017. Egypt and the levant in the early/Middle Bronze Age transition. In: Höflmayer, F. (Ed.), The Late Third Millennium in the Ancient near East: Chronology, C14 and Climate Change; Papers from the Oriental Institute Seminar Held at the Oriental Institute of the University of Chicago, 7–8 March 2014. Oriental Institute of the University of Chicago, Chicago.

Allcock, S.L., 2017. Long-term socio-environmental dynamics and adaptive cycles in Cappadocia, Turkey during the Holocene. Quat. Int. 446, 66–82.

Altaweel, M., Squitieri, A., 2018. Revolutionizing a World: from Small States to Universalism in the Pre-Islamic near East. UCL Press, London.

Attema, P., Bintliff, J., van Leusen, M., Bes, P., de Haas, T., Donev, D., Jongman, W., Kaptijn, E., Mayoral, V., Menchelli, S., Pasquinucci, M., Rosen, S., Sáánchez, J.G., Soler, L.G., Stone, D., Tol, G., Vermeulen, F., Vionis, A., 2020. A guide to good practice in mediterranean surface survey projects. Journal of Greek Archaeology 5, 1–62.

Bagg, A.M., 2013. Palestine under Assyrian rule: a new look at the Assyrian imperial policy in the west. J. Am. Orient. Soc. 133, 119–144.

Banning, E.B., 2007. Time and tradition in the transition from late Neolithic to Chalcolithic: summary and conclusions. Paleorient 33, 137–142.

Bar, S., 2013. Shifting settlement patterns in the Southern Jordan Valley and desert fringes of Samaria during the early Bronze Age I period. Palest. Explor. Q. 145, 90–107.

Bar, S., Zertal, A., 2021. The Manasseh Hill Country Survey Volume 6: the Eastern Samaria Shoulder, from Nahal Tirzah (Wadi Far'Ah) to Ma'Ale Ephraim Junction. Brill, Leiden.

Bar, S., Zertal, A., 2022. The Manasseh Hill Country Survey Volume 7: the South-Eastern Samaria Shoulder, from Wadi Rashash to Wadi 'Aujah. Brill, Leiden.

Bar-Matthews, M., Ayalon, A., 2011. Mid-holocene climate variations revealed by high-resolution speleothem records from Soreq Cave, Israel and their correlation with cultural changes. Holocene 21, 163–171.

Bar-Matthews, M., Ayalon, A., Gilmour, M., Matthews, A., Hawkesworth, C.J., 2003. Sea–land oxygen isotopic relationships from planktonic foraminifera and speleothems in the Eastern Mediterranean region and their implication for paleorainfall during interglacial intervals. Geochem. Cosmochim. Acta 67, 3181–3199.

Bar-Matthews, M., Ayalon, A., Kaufman, A., 1997. Late Quaternary paleoclimate in the Eastern Mediterranean Region from stable isotope analysis of speleothems at Soreq Cave, Israel. Quat. Res. 47, 155–168.

Bar-Matthews, M., Ayalon, A., Kaufman, A., 1998. Middle to late Holocene (6,500 yr. Period) paleoclimate in the Eastern Mediterranean Region from stable isotopic composition of speleothems from Soreq Cave, Israel. In: Issar, A.S., Brown, N. (Eds.), Water, Environment and Society in Times of Climatic Change: Contributions from an International Workshop Within the Framework of International Hydrological Program (IHP) UNESCO, Held at Ben-Gurion University, Sede Boker, Israel from 7–12 July 1996. Springer, Netherlands, Dordrecht, pp. 203–214.

Batist, Z., Roe, J., 2024. Open Archaeology, Open Source? Collaborative practices in an emerging community of archaeological software engineers. Internet Archaeol 67. https://doi.org/10.11141/ia.67.13.

Besnard, G., Khadari, B., Navascués, M., Fernández-Mazuecos, M., El Bakkali, A., Arrigo, N., Baali-Cherif, D., Brunini-Bronzini de Caraffa, V., Santoni, S., Vargas, P., Savolainen, V., 2013. The complex history of the olive tree: from late Quaternary diversification of Mediterranean lineages to primary domestication in the northern Levant. Proc. Biol. Sci. 280, 20122833.

Bevan, A., Crema, E.R., 2020. Modifiable reporting unit problems and time series of long-term human activity. Phil. Trans. Biol. Sci. 376, 20190726.

Bevan, A., Crema, E., Li, X., Palmisano, A., 2013. Intensities, interactions, and uncertainties: some new approaches to archaeological distributions. In: Computational Approaches to Archaeological Spaces. Routledge.

Bini, M., Zanchetta, G., Perşoiu, A., Cartier, R., Català, A., Cacho, I., Dean, J.R., Di Rita, F., Drysdale, R.N., Finnè, M., Isola, I., Jalali, B., Lirer, F., Magri, D., Masi, A., Marks, L., Mercuri, A.M., Peyron, O., Sadori, L., Sicre, M.-A., Welc, F., Zielhofer, C., Brisset, E., 2019. The 4.2 ka BP Event in the mediterranean region: an overview. Clim. Past 15, 555–577.

Bird, D., Miranda, L., Vander Linden, M., Robinson, E., Bocinsky, R.K., Nicholson, C., Capriles, J.M., Finley, J.B., Gayo, E.M., Gil, A., d'Alpoim Guedes, J., Hoggarth, J.A., Kay, A., Loftus, E., Lombardo, U., Mackie, M., Palmisano, A., Solheim, S., Kelly, R.L., Freeman, J., 2022. P3k14c, a synthetic global database of archaeological radiocarbon dates. Sci. Data 9, 27.

Braun, E., 2012. On some South Levantine early Bronze Age ceramic "Wares" and styles. Palest. Explor. Q. 144, 5–32.

Bronk Ramsey, C., 2017. Methods for summarizing radiocarbon datasets. Radiocarbon 59, 1809–1833.

Bronk Ramsey, C., Blaauw, M., Kearney, R., Staff, R.A., 2019. The importance of open access to chronological information: the IntChron initiative. Radiocarbon 61, 1121–1131.

Broshi, M., 1979. The population of Western Palestine in the roman-byzantine period. Bull. Am. Sch. Orient. Res. 1–10.

Broshi, M., Finkelstein, I., 1992. The population of Palestine in Iron Age II. Bull. Am. Sch. Orient. Res. 47–60.

Broshi, M., Gophna, R., 1984. The settlements and population of Palestine during the early Bronze Age II-III. Bull. Am. Sch. Orient. Res. 41–53.

Broshi, M., Gophna, R., 1986. Middle Bronze Age II Palestine: its settlements and population. Bull. Am. Sch. Orient. Res. 73–90.

Brown, W.A., 2017. The past and future of growth rate estimation in demographic temporal frequency analysis: biodemographic interpretability and the ascendance of dynamic growth models. J. Archaeol. Sci. 80, 96–108.

Bunbury, M.M.E., Austvoll, K.I., Jørgensen, E.K., Nielsen, S.V., Kneisel, J., Weinelt, M., 2023. Understanding climate resilience in Scandinavia during the Neolithic and early Bronze Age. Quat. Sci. Rev. 322, 108391.

Bunimovitz, S., 1998. On the edge of empires - the late Bronze Age. In: Levy, T.E. (Ed.), The Archaeology of Society on the Holy Land. Leicester University Press, London.

Capriles, J.M., 2023. The Bolivian radiocarbon database: a countrywide compilation of radiocarbon dates. J. Open Archaeol. Data 11, 6.

Casana, J., 2007. Structural transformations in settlement systems of the Northern levant. Am. J. Archaeol. 111, 195–221.

Cassis, M., Doonan, O., Elton, H., Newhard, J., 2018. Evaluating archaeological evidence for demographics, abandonment, and recovery in late Antique and byzantine Anatolia. Hum. Ecol. 46, 381–398.

Cheng, H., Sinha, A., Verheyden, S., Nader, F.H., Li, X.L., Zhang, P.Z., Yin, J.J., Yi, L., Peng, Y.B., Rao, Z.G., Ning, Y.F., Edwards, R.L., 2015. The climate variability in northern Levant over the past 20,000 years. Geophys. Res. Lett. 42, 8641–8650.

Cherry, J.F., 1983. Frogs around the pond: perspectives on current archaeological survey projects in the mediterranean region. In: Keller, D.R., Rupp, D.W. (Eds.), Archaeological Survey in the Mediterranean Area. Oxford, pp. 375–416.

Chesson, M.S., 2018. The Southern levant during the early Bronze Age I–III. In: Yasur-Landau, A., Cline, E.H., Rowan, Y.M. (Eds.), The Social Archaeology of the Levant: from Prehistory to the Present. Cambridge University Press, Cambridge.

Clarke, J., Brooks, N., Banning, E.B., Bar-Matthews, M., Campbell, S., Clare, L., Cremaschi, M., di Lernia, S., Drake, N., Gallinaro, M., Manning, S., Nicoll, K., Philip, G., Rosen, S., Schoop, U.-D., Tafuri, M.A., Weninger, B., Zerboni, A., 2016. Climatic changes and social transformations in the Near East and North Africa during the "long" 4th millennium BC: a comparative study of environmental and archaeological evidence. Quat. Sci. Rev. 136, 96–121.

Cohen, S.L., 2013. The Southern levant (Cisjordan) during the middle Bronze Age. In: Killebrew, A.E., Steiner, M. (Eds.), Oxford Handbook of Ancient Anatolian Studies.

Cohen, S.L., 2018. Continuity, innovation, and change: the intermediate Bronze Age in the Southern levant. In: Yasur-Landau, A., Cline, E.H., Rowan, Y.M. (Eds.), The Social Archaeology of the Levant: from Prehistory to the Present. Cambridge University Press, Cambridge, pp. 183–198.

Cookson, E., Hill, D.J., Lawrence, D., 2019. Impacts of long term climate change during the collapse of the akkadian Empire. J. Archaeol. Sci. 106, 1–9.

Crema, E.R., 2012. Modelling temporal uncertainty in archaeological analysis. J. Archaeol. Method Theor 19, 440–461.

Crema, E.R., 2022. Statistical Inference of Prehistoric Demography from Frequency Distributions of Radiocarbon Dates: a Review and a Guide for the Perplexed, pp. 1387–1418.

Crema, E.R., Bevan, A., Lake, M.W., 2010. A probabilistic framework for assessing spatio-temporal point patterns in the archaeological record. J. Archaeol. Sci. 37, 1118–1130.

Crema, E.R., Habu, J., Kobayashi, K., Madella, M., 2016. Summed probability distribution of 14C dates suggests regional divergences in the population dynamics of the Jomon period in Eastern Japan. PLoS One 11, e0154809.

Crema, E.R., Kobayashi, K., 2020. A multi-proxy inference of Jōmon population dynamics using bayesian phase models, residential data, and summed probability distribution of 14C dates. J. Archaeol. Sci. 117, 105136.

Crema, E.R., Shoda, S., 2021. A Bayesian approach for fitting and comparing demographic growth models of radiocarbon dates: a case study on the Jomon-Yayoi transition in Kyushu (Japan). PLoS One 16, e0251695.

Cumming, G.S., Peterson, G.D., 2017. Unifying research on social–ecological resilience and collapse. Trends Ecol. Evol. 32, 695–713.

Dagan, Y., 1979. Survey, Shephelah. Hadashot Arkheologiyot, pp. 30–32 (in Hebrew).

Davidovich, U., 2012. The early bronze IB in the Judean desert Caves. Tel Aviv 39, 3–19.

Davidovich, U., 2013. The chalcolithic – early Bronze Age transition: a view from the Judean desert Caves, Southern levant. Paleorient 39, 125–138.

de Miroschedji, P., 2013. The Southern levant (Cisjordan) during the early Bronze Age. In: Killebrew, A.E., Steiner, M. (Eds.), The Oxford Handbook of the Archaeology of the Levant: C. 8000-332 BCE. Oxford University Press, Oxford.

Drennan, R.D., Berrey, C.A., Peterson, C.E., 2015. Regional Settlement Demography in Archaeology. Eliot Werner Publications.

Edelstein, G., Milevski, I., Aurant, S., 1998. Terraces and stone mounds. In: Gitler, G. Edelstein I. Milevski S. Aurant H., Horwitz, L.K., Reich, M.E. Kislev R., Rosen, A.M., Siegal, S.A. Rosen S., Smith, P. (Eds.), Villages, Terraces and Stone Mounds: Excavations at Manahat, Jerusalem, 1987-1989. Israel Antiquities Authority, pp. 6–13.

Falconer, S.E., Savage, S.H., 2009. The Bronze Age political landscape of the Southern levant. In: Falconer, S.E., Redman, C.L. (Eds.), Polities and Power: Archaeological Perspectives on the Landscapes of Early States. University of Arizona Press, pp. 125–161.

Fantalkin, A., Tal, O., 2009. Re-Discovering the Iron Age fortress at Tell Qudadi in the context of neo-assyrian imperialistic policies. Palest. Explor. Q. 141, 188–206.

Faust, A., 2003. Judah in the sixth century B. C. E.: a rural perspective. Palest. Explor. Q. 135, 37–53.

Faust, A., 2007. Settlement dynamics and demographic fluctuations in Judah from the late Iron Age to the Hellenistic Period and the archaeology of Persian-Period Yehud. Library of Second Temple Studies 65, 23.

Faust, A., 2008. Settlement and demography in seventh-century judah and the extent and intensity of Sennacherib's campaign. Palest. Explor. Q. 140, 168–194.

Faust, A., 2013. The shephelah in the Iron Age: a new look on the settlement of Judah. Palest. Explor. Q. 145, 203–219.

Faust, A., 2015. Settlement, economy, and demography under Assyrian rule in the west: the territories of the former kingdom of Israel as a Test case. J. Am. Orient. Soc. 135, 765–789.

Faust, A., 2018. A social archaeology of the Kingdom of Judah Tenth–sixth Centuries bce. In: Yasur-Landau, A., Cline, E.H., Rowan, Y.M. (Eds.), The Social Archaeology of the Levant: from Prehistory to the Present. Cambridge University Press, Cambridge, pp. 337–353.

Faust, A., 2021. The Neo-Assyrian Empire in the Southwest: Imperial Domination and Its Consequences. Oxford University Press, Oxford.

Feeser, I., Dörfler, W., Kneisel, J., Hinz, M., Dreibrodt, S., 2019. Human impact and population dynamics in the Neolithic and Bronze Age: Multi-proxy evidence from north-western Central Europe. Holocene 29, 1596–1606.

Finkelstein, I., 1992. Horvat qitmit and the Southern trade in the late Iron Age II. Zeitschrift des Deutschen Palaestina-Vereins (1953-) 108, 156–170.

Finkelstein, I., 1996a. The philistine countryside. Isr. Explor. J. 225–242.

Finkelstein, I., 1996b. The Territorio-Political System of canaan in the late Bronze Age. Ugarit-Forschungen 221–255.

Finkelstein, I., 1998. The great transformation: the “Conquest” of the highlands frontiers and the rise of the territorial States. In: Levy, T.E. (Ed.), The Archaeology of Society in the Holy Land, pp. 349–365. London.

Finkelstein, I., 2003. Finkelstein, I. 2003. City states and states: polity dynamics in the 10th-9th centuries B.C.E. In: Dever, W.G., Gitin, S. (Eds.), Symbiosis, Symbolism and the Power of the Past: Canaan, Ancient Israel, and Their Neighbors. Winona Lake, pp. 75–83.

Finkelstein, I., 2011. Observations on the layout of Iron Age samaria. Tel Aviv 38, 194–207.

Finkelstein, I., 2018. Jerusalem in the Iron Age: archaeology and text; reality and myth. In: Galor, K., Avni, G. (Eds.), *The Jerusalem Perspective: 150 Years of Archaeological Research in the Holy City*, Eisenbrauns, Winona Lake, pp. 189–201.

Finkelstein, I., Adams, M.J., Dunseth, Z.C., Shahack-Gross, R., 2018. The archaeology and history of the negev and neighbouring areas in the third millennium BCE: a new paradigm. Tel Aviv 45, 63–88.

Finkelstein, I., Gadot, Y., Langgut, D., 2022. The unique specialised economy of Judah under Assyrian rule and its impact on the material culture of the kingdom. Palest. Explor. Q. 154, 261–279.

Finkelstein, I., Gophna, R., 1993. Settlement, demographic, and economic patterns in the highlands of Palestine in the chalcolithic and early bronze periods and the beginning of urbanism. Bull. Am. Sch. Orient. Res. 1–22.

Finkelstein, I., Langgut, D., 2014. Dry climate in the middle bronze I and its impact on settlement patterns in the levant and beyond: new pollen evidence. J. Near E. Stud. 73, 219–234.

Finkelstein, I., Lederman, Z., Bunimovitz, S., 1997. Highlands of Many Cultures: the Southern Samaria Survey ; the Sites. Institute of Archaeology of Tel-Aviv University, Publications Section, Tel Aviv.

Finkelstein, I., Piasetzky, E., 2010. The Iron I/IIA transition in the levant: a reply to Mazar and Bronk ramsey and a new perspective. radiocarbon. an international journal of cosmogenic isotope research 52, 1667–1680.

Finkelstein, I., Piasetzky, E., 2011. The Iron Age chronology debate: is the gap narrowing? Near E. Archaeol. 74, 50–54.

Finné, M., Woodbridge, J., Labuhn, I., Roberts, C.N., 2019. Holocene hydro-climatic variability in the Mediterranean: a synthetic multi-proxy reconstruction. Holocene 29, 847–863.

Fleitmann, D., Burns, S.J., Mangini, A., Mudelsee, M., Kramers, J., Villa, I., Neff, U., Al-Subbary, A.A., Buettner, A., Hippler, D., Matter, A., 2007. Holocene ITCZ and Indian monsoon dynamics recorded in stalagmites from Oman and Yemen (Socotra). Quat. Sci. Rev. 26, 170–188.

Flohr, P., Fleitmann, D., Matthews, R., Matthews, W., Black, S., 2016. Evidence of resilience to past climate change in Southwest Asia: early farming communities and the 9.2 and 8.2 ka events. Quat. Sci. Rev. 136, 23–39.

Flohr, P., Fleitmann, D., Zorita, E., Sadekov, A., Cheng, H., Bosomworth, M., Edwards, L., Matthews, W., Matthews, R., 2017. Late Holocene droughts in the Fertile Crescent recorded in a speleothem from northern Iraq. Geophys. Res. Lett. 44, 1528–1536.

French, J.C., 2015. The demography of the Upper Palaeolithic hunter–gatherers of Southwestern France: a multi-proxy approach using archaeological data. J. Anthropol. Archaeol. 39, 193–209.

French, J.C., Riris, P., Pablo, J. F.-L. de, Lozano, S., Silva, F., 2021. A manifesto for palaeodemography in the twenty-first century. Philos. Trans. R. Soc. B 376, 1816.

Frumkin, A., Ford, D.C., Schwarcz, H.P., 1999. Continental oxygen isotopic record of the last 170,000 years in Jerusalem. Quat. Res. 51, 317–327.

Goldberg, P., Rosen, A.M., 1987. Early Holocene paleoenvironments of Israel. In: Levy, T. E. (Ed.), Shiqmim I. Archeopress, Oxford.

Golden, J.M., 2009. Dawn of the Metal Age: Technology and Society During the Levantine Chalcolithic. Routledge & CRC Press.

Gophna, R., Paz, Y., 2014. From village to town to village again: settlementdynamics in the central coastal Plain and AdjacentShephelah from the late early Bronze Age I to EarlyBronze Age III. Strata: Bulletin of the Anglo-Israel Archaeolocial Society 32, 13–35.

Gophna, R., Portugali, J., 1988. Settlement and demographic processes in Israel's coastal Plain from the chalcolithic to the middle Bronze Age. Bull. Am. Sch. Orient. Res. 11–28.

Goren, Y., 2014. GODS, CAVES, and SCHOLARS: chalcolithic cult and metallurgy in the Judean desert. Near E. Archaeol. 77, 4, 260-266.

Greenberg, R., 2013. Introduction to the levant during the early Bronze Age. In: Killebrew, E., Steiner, M. (Eds.), The Oxford Handbook of the Archaeology of the Levant: C. 8000-332 BCE. Oxford University Press.

Greenberg, R., 2017. No collapse: transmutations of early Bronze Age urbanism in the Southern Levant. In: Höflmayer, F. (Ed.), The Late Third Millennium in the Ancient near East: Chronology, C14 and Climate Change; Papers from the Oriental Institute Seminar Held at the Oriental Institute of the University of Chicago, 7–8 March 2014. Oriental Institute of the University of Chicago, Chicago, pp. 33–60.

Greenberg, R., 2019. The Archaeology of the Bronze Age Levant: from Urban Origins to the Demise of City-States, 3700–1000 BCE. Cambridge University Press, Cambridge.

Greenberg, R., Keinan, A., 2009. Israeli Archaeological Activity in the West Bank 1967-2007: a Sourcebook. Ostracon, Jerusalem.

Greener, A., Finkelstein, I., Langgut, D., 2018. Settlement oscillations along the desert fringes of the Southern Levant: impact of climate versus economic and historical factors. Ugarit-Forschungen 49, 165-196.

Grigson, G., 1998. Plough and pasture in the early economy of the southern Levant. In: Levy, T.E. (Ed.), The Archaeology of Society in the Holy Land. Leicester University Press, London, pp. 245–268.

Hauptmann, A., 2003. Developments in copper metallurgy during the fourth and third millennia BC at Feinan, Jordan. In: Craddock, P.T., Lang, J. (Eds.), Mining and Metal Production Through the Ages. British Museum Press, London, pp. 90–100.

Hazell, C.J., Pound, M.J., Hocking, E.P., 2022. High-resolution Bronze Age palaeoenvironmental change in the Eastern Mediterranean: exploring the links between climate and societies. Palynology 46, 1–20.

Herzog, Z., Singer-Avitz, L., 2006. Sub-Dividing the Iron Age IIA in Northern Israel: a suggested solution to the chronological debate. Tel Aviv 33, 163–195.

Hinz, M., Furholt, M., Müller, J., Rinne, C., Raetzel-Fabian, D., Sjögren, K.-G., Wotzka, H.-P., 2012. RADON - Radiocarbon dates online 2012. Central European database of 14C dates for the Neolithic and the early Bronze Age. Journal of Neolithic Archaeology 2012, 65.

Hoggarth, J.A., Ebert, C.E., Castelazo-Calva, V.E., 2021. MesoRAD: a new radiocarbon data set for archaeological research in mesoamerica. J. Open Archaeol. Data 9, 10.

Horwitz, L.K., 1989. Diachronic Changes in Rural Husbandry Practices in Bronze Age Settlements from the Refaim Valley, Israel. Palestine Exploration Quarterly.

Ilan, D., 1998. The dawn of internationalism - the middle Bronze Age. In: Levy, T.E. (Ed.), The Archaeology of Society on the Holy Land. Leicester University Press, London.

Ilan, D., 2018. The “conquest” of the Highlands in the Iron Age I. In: Yasur-Landau, A., Cline, E.C., Rowan, Y.M. (Eds.), The Social Archaeology of the Levant: from Prehistory to the Present. Cambridge University Press, Cambridge, pp. 283–309.

Jasmine, M., 2006. The political organization of the city-states in Southwestern Palestine in the late Bronze Age IIB. In: Maeir, A.M., de Miroschedji, P. (Eds.), *I Will Speak the Riddles of Ancient Times: Archaeological and Historical Studies in Honor of Amihai Mazar on the Occasion of His Sixtieth Birthday*, Eisenbrauns, Winona Lake.

Johnson, I., 2004. Aoristic Analysis: Seeds of a New Approach to Mapping Archaeological Distributions Through Time.

Jones, M.D., Abu-Jaber, N., AlShdaifat, A., Baird, D., Cook, B.I., Cuthbert, M.O., Dean, J. R., Djamali, M., Eastwood, W., Fleitmann, D., Haywood, A., Kwiecien, O., Larsen, J., Maher, L.A., Metcalfe, S.E., Parker, A., Petrie, C.A., Primmer, N., Richter, T., Roberts, N., Roe, J., Tindall, J.C., Ünal-İmer, E., Weeks, L., 2019. 20,000 years of societal vulnerability and adaptation to climate change in southwest Asia. WIREs Water 6.

Kaniewski, D., Marriner, N., Bretschneider, J., Jans, G., Morhange, C., Cheddadi, R., Otto, T., Luce, F., Van Campo, E., 2019. 300-Year drought frames late Bronze Age to early Iron Age transition in the Near East: new palaeoecological data from Cyprus and Syria. Reg. Environ. Change 19, 2287-2297.

Katsianis, M., Bevan, A., Styliaras, G., Maniatis, Y., 2020. An aegean history and archaeology written through. Radiocarbon Dates Journal of Open Archaeology Data 8, 5.

Keinan-Schoonbaert, A., 2016. Multiple inventories and divided archaeology in the West Bank: an assessment of databases in the Etzion Bloc. J. Field Archaeol. 41, 645–659.

Keinan-Schoonbaert, A., 2018. The West bank and East Jerusalem archaeological database: narratives of archaeology and archaeological practices. In: Levy, T.E., Jones, I.W.N. (Eds.), Cyber-Archaeology and Grand Narratives. Digital Technology and Deep-Time Perspectives on Culture Change in the Middle East. Springer International Publishing, Cham, pp. 123–141.

Kelly, R.L., Mackie, M.E., Robinson, E., Meyer, J., Berry, M., Boulanger, M., Codding, B. F., Freeman, J., Garland, C.J., Gingerich, J., Hard, R., Haug, J., Martindale, A., Meeks, S., Miller, M., Miller, S., Perttula, T., Railey, J.A., Reid, K., Scharlotta, I., Spangler, J., Thomas, D.H., Thompson, V., White, A., 2022. A new radiocarbon database for the lower 48 States. Am. Antiq. 87, 581–590.

Killebrew, A.E., 2013. Israel during the iron age II period. In: Killebrew, E., Steiner, M. (Eds.), The Oxford Handbook of the Archaeology of the Levant: C. 8000-332 BCE. Oxford University Press.

Kolář, J., Macek, M., Tkáč, P., Novák, D., Abraham, V., 2022. Long-term demographic trends and spatio-temporal distribution of past human activity in Central Europe: comparison of archaeological and palaeoecological proxies. Quat. Sci. Rev. 297, 107834.

Kolář, J., Macek, M., Tkáč, P., Szabó, P., 2016. Spatio-Temporal modelling as A way to reconstruct patterns of past human activities. Archaeometry: bulletin of the research laboratory for archaeology and the history of art 58, 513–528 oxford university.

Kudo, Y., Sakamoto, M., Hakozaki, M., Stevens, C.J., Crema, E.R., 2023. An archaeological radiocarbon database of Japan. J. Open Archaeol. Data 11, 11.
Labuhn, I., Finné, M., Izdebski, A., Roberts, N., Woodbridge, J., 2016. Climatic changes and their impacts in the Mediterranean during the first millennium AD. Late Antiq. Archaeol. 12, 65–88.
Langgut, D., Adams, M.J., Finkelstein, I., 2016. Climate, settlement patterns and olive horticulture in the southern Levant during the Early Bronze and Intermediate Bronze Ages (c. 3600–1950 BC). Levant 48, 117–134.
Langgut, D., Cheddadi, R., Carrión, J.S., Cavanagh, M., Colombaroli, D., Eastwood, W.J., Greenberg, R., Litt, T., Mercuri, A.M., Miebach, A., Roberts, C.N., Woldring, H., Woodbridge, J., 2019. The origin and spread of olive cultivation in the Mediterranean Basin: the fossil pollen evidence. Holocene 29, 902–922.
Langgut, D., Finkelstein, I., 2023. Paleo-environment of the Southern levant during the bronze and iron ages. The pollen evidence. In: Lipschits, I. Koch O., Sergi, O. (Eds.), From Nomadism to Monarchy?: Revisiting the Early Iron Age Southern Levant. Penn State University Press, pp. 7–28.
Langgut, D., Finkelstein, I., Litt, T., Neumann, F.H., Stein, M., 2015. Vegetation and climate changes during the bronze and iron ages (3600–600 BCE) in the Southern levant based on palynological records. Radiocarbon 57, 217–235.
Langgut, D., Lipschits, O., 2017. Dry climate during the early Persian period and its impact on the establishment of idumea. Transeuphratène 135–162.
Langgut, D., Neumann, F.H., Stein, M., Wagner, A., Kagan, E.J., Boaretto, E., Finkelstein, I., 2014. Dead Sea pollen record and history of human activity in the Judean Highlands (Israel) from the Intermediate Bronze into the Iron Ages (2500–500 BCE). Palynology 38, 280–302.
Lawrence, D., Palmisano, A., de Gruchy, M.W., 2021. Collapse and continuity: a multi-proxy reconstruction of settlement organization and population trajectories in the Northern Fertile Crescent during the 4.2kya Rapid Climate Change event. PLoS One 16, e0244871.
Lawrence, D., Philip, G., de Gruchy, M.W., 2022. Climate change and early urbanism in Southwest Asia: a review. WIREs Clim. Change 13, e741.
Lawrence, D., Philip, G., Hunt, H., Snape-Kennedy, L., Wilkinson, T.J., 2016. Long term population, City size and climate trends in the fertile crescent: a first approximation. PLoS One 11, e0152563.
Levy, T.E., 1998. Cult, metallurgy and rank societies - chalcolithic period (Ca. 4500 - 3500 BCE). In: Levy, T.E. (Ed.), The Archaeology of Society in the Holy Land. Leicester University Press, London, pp. 226–244.
Levy, T.E., Burton, M.M., Rowan, Y.M., 2006. Chalcolithic hamlet excavations near Shiqmim, Negev Desert, Israel. J. Field Archaeol. 31, 41–60.
Levy, T.E., Shalev, S., 1989. Prehistoric metalworking in the southern Levant: archaeometallurgical and social perspectives. World Archaeol. 20, 352-372.
Litt, T., Ohlwein, C., Neumann, F.H., Hense, A., Stein, M., 2012. Holocene climate variability in the Levant from the Dead Sea pollen record. Quat. Sci. Rev. 49, 95–105.
Liverani, M., 1988. The growth of the Assyrian Empire in the Habur/Middle euphrates area: a new paradigm. State Archives of Assyria Bulletin II, 81–98.
Liverani, M., 2003. Oltre La Bibbia. Storia Antica Di Israele. Laterza.
Liverani, M., 2014. Israel's History and the History of Israel. Routledge, Taylor & Francis Group, London New York.
Loftus, E., Mitchell, P.J., Ramsey, C.B., 2019. An archaeological radiocarbon database for southern Africa. Antiquity 93, 870–885.
Lucarini, G., Wilkinson, T., Crema, E.R., Palombini, A., Bevan, A., Broodbank, C., 2020. The MedAfriCarbon radiocarbon database and web application. Archaeological dynamics in Mediterranean Africa, ca. 9600–700. BC Journal of Open Archaeology Data 8, 1.
Marchetti, N., Bortolini, E., Menghi Sartorio, J.C., Orrù, V., Zaina, F., 2025. Long-Term urban and population trends in the Southern mesopotamian floodplains. J. Archaeol. Res. 33, 117–158.
Marston, J.M., 2023. Modeling resilience and sustainability in Ancient agricultural systems. J. Ethnobiol. 35, 3, 585-605.
Mashiach, A., Davidovich, U., 2023. The En-Gedi Spring site and the judahite expansion into the Judaean desert in the late Iron Age. Tel Aviv 50, 21–43.
Mazar, A., 2011. The Iron Age chronology debate: is the gap narrowing? Another viewpoint. Near E. Archaeol. 74, 105–111.
Mazar, ʿAmiḥai (Ed.), 2009. Archaeology of the Land of the Bible, vol. 1. Yale University Press, New Haven, Conn London, 10.000 - 586 B.C.E./by Amihai Mazar.
Mazar, A., Ramsey, C.B., 2008. 14C dates and the Iron Age chronology of Israel: a response. Radiocarbon 50, 159–180.
Mazar, A., Ramsey, C.B., 2010. A response to Finkelstein and Piasetzky'S criticism and "New Perspective". Radiocarbon 52, 1681–1688.
McLaughlin, T.R., 2019. On applications of space–time modelling with open-source 14C Age calibration. J. Archaeol. Method Theor 26, 479–501.
Nigro, L., Calcagnile, L., Yasin, J., Gallo, E., Quarta, G., 2019. Jericho and the chronology of Palestine in the early bronze age: a radiometric re-assessment. radiocarbon. an international journal of cosmogenic isotope research 61, 211–241.
Orland, I.J., Bar-Matthews, M., Ayalon, A., Matthews, A., Kozdon, R., Ushikubo, T., Valley, J.W., 2012. Seasonal resolution of Eastern Mediterranean climate change since 34 ka from a Soreq Cave speleothem. Geochem. Cosmochim. Acta 89, 240–255.
Orton, D., Morris, J., Pipe, A., 2017. Catch per unit research effort: sampling intensity, chronological uncertainty, and the onset of marine fish consumption. Historic London 3, 1.
Palmisano, A., 2023. Inferring population dynamics from multiple archaeological proxies: an overview of methods and challenges. In: Belvedere, O., Bergemann, J. (Eds.), Archaeology and Historical Demography. Methods and Case Studies Between Mediterranean and Central Europe. Verlag Marie Leidorf GmbH, pp. 25–41.
Palmisano, A., Bevan, A., Kabelindde, A., Roberts, N., Shennan, S., 2021a. Long-Term demographic trends in prehistoric Italy: climate impacts and regionalised socio-ecological trajectories. J. World PreHistory 34, 381–432.
Palmisano, A., Bevan, A., Kabelindde, A., Roberts, N., Shennan, S., 2022a. AIDA (Archive of Italian Radiocarbon Dates).
Palmisano, A., Bevan, A., Lawrence, D., Shennan, S., 2022b. The NERD dataset: near east radiocarbon dates between 15,000 and 1,500 cal. Yr. BP. J. Open Archaeol. Data 10, 2.
Palmisano, A., Bevan, A., Shennan, S., 2017. Comparing archaeological proxies for long-term population patterns: an example from central Italy. J. Archaeol. Sci. 87, 59–72.
Palmisano, A., Lawrence, D., de Gruchy, M.W., Bevan, A., Shennan, S., 2021b. Holocene regional population dynamics and climatic trends in the Near East: a first comparison using archaeo-demographic proxies. Quat. Sci. Rev. 252, 106739.
Palmisano, A., Squitieri, A., 2023. Review of the Neo-Assyrian Empire in the Southwest: imperial domination and its consequences by Avraham Faust. Bull. Am. Sch. Orient. Res. 389, 235–238.
Palmisano, A., Titolo, A., 2024. The good, the bad and the ugly: evaluating Open Science practices in archaeology. Archeologia e Calcolatori 35, 75–84.
Palmisano, A., Woodbridge, J., Roberts, C.N., Bevan, A., Fyfe, R., Shennan, S., Cheddadi, R., Greenberg, R., Kaniewski, D., Langgut, D., Leroy, S.A.G., Litt, T., Miebach, A., 2019. Holocene landscape dynamics and long-term population trends in the levant. Holocene 29, 708–727.
Panitz-Cohen, N., 2013. The Southern levant (Cisjordan) during the late Bronze Age. In: The Oxford Handbook of the Archaeology of the Levant: C. 8000-332 BCE. Oxford University Press, Oxford.
Pardo-Gordó, S., Vidal-Matutano, P., González-Marrero, M. del C. and Chávez-Álvarez, M. E. (2023). The 14Canarias web application. An interactive radiocarbon database for the Canary Islands. Journal of Open Archaeology Data 11, 4.
Parker, B.J., 2001. The Mechanics of Empire: the Northern Frontier of Assyria as a Case Study in Imperial Dynamics. Helsinki.
Petchey, F., Bickler, S., Hughes, L., Bunbury, M., 2022. The Aotearoa/New Zealand radiocarbon database upgrade. Archaeol. N. Z. 65, 32–40.
Philip, G., 2003. The early Bronze Age of the Southern levant: a landscape approach. J. Mediterr. Archaeol. 16, 103–132.
Rademaker, K., 2024. Updated Peru archaeological radiocarbon database, 20,000–7000 14C BP. Quat. Int. 703, 32–48.
Radner, K., 2006. Provinz C. Reallexikon der Assyriologie und Vorderasiatischen Archäologie 11, 42–68.
Radner, K., 2008. Esarhaddon's expedition from Palestine to Egypt in 671 BCE: a trek through Negev and Sinai. In: Czichon, D. Bonatz R., Kreppner, F.J. (Eds.), Fundstellen: Gesammelte Schriften Zur Archäologie Und Geschichte Altvorderasiens Ad Honorem Hartmut Kühne. Harrassowitz, Wiesbaden, pp. 305–314.
Ratcliffe, J.H., 2000. Aoristic analysis: the spatial interpretation of unspecific temporal events. Int. J. Geogr. Inf. Sci. 14, 669–679.
Rayne, L., Gatto, M.C., Abdulaati, L., Al-Haddad, M., Sterry, M., Sheldrick, N., Mattingly, D., 2020. Detecting change at archaeological sites in North Africa using open-source satellite imagery. Remote Sens. 12, 3694, 3694.
Regev, J., Gadot, Y., Roth, H., Uziel, J., Chalaf, O., Ben-Ami, D., Mintz, E., Regev, L., Boaretto, E., 2021. Middle Bronze Age Jerusalem: recalculating its character and chronology. Radiocarbon 63, 853–883.
Regev, J., Miroschedji, P.D., Greenberg, R., Braun, E., Greenhut, Z., Boaretto, E., 2012. Chronology of the early Bronze Age in the Southern levant: new analysis for a high chronology. radiocarbon. an international journal of cosmogenic isotope research 54, 525–566.
Rick, J.W., 1987. Dates as data: an examination of the Peruvian preceramic radiocarbon record. Am. Antiq. 52, 55–73.
Roberts, C.N., Woodbridge, J., Palmisano, A., Bevan, A., Fyfe, R., Shennan, S., 2019. Mediterranean landscape change during the Holocene: synthesis, comparison and regional trends in population, land cover and climate. Holocene 29, 923–937.
Roberts, N., 2021. Boon or curse? The role of climate change in the rise and demise of anatolian civilizations. In: Roosevelt, Christopher H., Haldon, John (Eds.), WINDS OF CHANGE Environment and Society in Anatolia, pp. 5–35.
Roberts, N., Cassis, M., Doonan, O., Eastwood, W., Elton, H., Haldon, J., Izdebski, A., Newhard, J., 2018. Not the end of the world? Post-Classical decline and recovery in rural Anatolia. Hum. Ecol. 46, 305–322.
Roberts, N., Eastwood, W.J., Kuzucuoğlu, C., Fiorentino, G., Caracuta, V., 2011. Climatic, vegetation and cultural change in the eastern Mediterranean during the mid-holocene environmental transition. Holocene 21, 147–162.
Roberts, N., Jones, M.D., Benkaddour, A., Eastwood, W.J., Filippi, M.L., Frogley, M.R., Lamb, H.F., Leng, M.J., Reed, J.M., Stein, M., Stevens, L., Valero-Garcés, B., Zanchetta, G., 2008. Stable isotope records of late Quaternary climate and hydrology from Mediterranean lakes: the ISOMED synthesis. Quat. Sci. Rev. 27, 2426–2441.
Robles, M., Peyron, O., Brugiapaglia, E., Ménot, G., Dugerdil, L., Ollivier, V., Ansanay-Alex, S., Develle, A.-L., Tozalakyan, P., Meliksetian, K., Sahakyan, K., Sahakyan, L., Perello, B., Badalyan, R., Colombié, C., Joannin, S., 2022. Impact of climate changes on vegetation and human societies during the Holocene in the South Caucasus (Vanevan, Armenia): a multiproxy approach including pollen, NPPs and brGDGTs. Quat. Sci. Rev. 277, 107297.
Roe, J., Hinz, M., 2022. XRONOS: an open repository and curation platform for chronometric data. In: Caa 2022. Oxford.
Roe, J., Schmid, C., Ebrahimiabareghi, S., Heitz, C., Hinz, M., 2025. XRONOS: an Open Data Infrastructure for Archaeological Chronology.
Rosen, A.M., Rivera-Collazo, I., 2012. Climate change, adaptive cycles, and the persistence of foraging economies during the late Pleistocene/Holocene transition in the Levant. Proc. Natl. Acad. Sci. 109, 3640–3645.

Rosen, S., 2008. Desert pastoral nomadism in the longue durée: a case Study from the negev and the Southern Levantine deserts. In: Barnard, H., Wendrich, W. (Eds.), The Archaeology of Mobility: Old World and New World Nomadism. Cotsen Institute of Archaeology Press, Los Angeles, pp. 115–140.
Rosen, S.A., 1987. Demographic trends in the negev highlands: Preliminary Results from the Emergency Survey. Bull. Am. Sch. Orient. Res. 45–58.
Rosen, S.A., 2011. The desert and the pastoralist: an archaeological perspective on human-landscape interaction in the negev over the millennia. Ann. Arid Zone 50.
Rosenzweig, M.S., Marston, J.M., 2018. Archaeologies of Empire and environment. J. Anthropol. Archaeol. 52, 87–102.
Rowan, Y.M., 2013. The Southern levant (Cisjordan) during the chalcolithic period. In: Killebrew, A.E., Steiner, M. (Eds.), The Oxford Handbook of the Archaeology of the Levant: C. 8000-332 BCE. Oxford University Press, Oxford.
Rowan, Y.M., 2018. The spiritual and social landscape during the chalcolithic period. In: Yasur-Landau, A., Cline, E.C., Rowan, Y.M. (Eds.), The Social Archaeology of the Levant: from Prehistory to the Present. Cambridge University Press, Cambridge, pp. 122–145.
Rowan, Y.M., Golden, J., 2009. The chalcolithic period of the Southern levant: a synthetic review. J. World PreHistory 22, 1–92.
Sapir-Hen, L., 2017. Pax Assyriaca and the animal economy in the Southern levant:: regional and local-scale imperial contacts. *Rethinking Israel: studies in the history and archaeology of Ancient Israel in honor of Israel Finkelstein*. Eisenbrauns, Winona Lake 343–355.
Savage, S.H., Falconer, S.E., 2003. Spatial and statistical inference of late Bronze Age polities in the Southern levant. Bull. Am. Sch. Orient. Res. 330, 31–45.
Schmid, C., Seidensticker, D., Hinz, M., 2019. c14bazAAR: an R package for downloading and preparing C14 dates from different source databases. J. Open Source Softw. 4, 1914.
Sergi, O., 2023. The kingdoms of Israel and Judah. In: Moeller, K. Radner N., Potts, D.T. (Eds.), The Oxford History of the Ancient near East Volume IV: the Age of Assyria the Oxford History of the Ancient near East Volume IV: the Age of Assyria. Oxford University Press, 0.
Shah, A., Morrill, C., Gille, E., Gross, W., Anderson, D., Bauer, B., Buckner, R., Hartman, M., 2013. Global speleothem oxygen isotope measurements since the last glacial maximum. Dataset Papers in Science 2013.
Sharon, I., 2013. Levantine chronology. In: Killebrew, E., Steiner, M. (Eds.), The Oxford Handbook of the Archaeology of the Levant: C. 8000-332 BCE. Oxford University Press.
Shennan, S., Sear, R., 2020. Archaeology, demography and life history theory together can help us explain past and present population patterns. Phil. Trans. Biol. Sci. 376, 20190711.
Singer, A., 2007. The Soils of Israel. Springer, Berlin, Heidelberg.
Sinha, A., Kathayat, G., Weiss, H., Li, H., Cheng, H., Reuter, J., Schneider, A.W., Berkelhammer, M., Adalı, S.F., Stott, L.D., Edwards, R.L., 2019. Role of climate in the rise and fall of the Neo-Assyrian Empire. Sci. Adv. 5 eaax6656.
Squitieri, A., 2024. Assyrian conquest and ruralization: unveiling territorial dynamics in the provinces of Magiddû and samerina. Levant 56, 239–258.
Suriano, M., 2013. Historical geography of the Ancient levant. In: Killebrew, A.E., Steiner, M. (Eds.), The Oxford Handbook of the Archaeology of the Levant: C. 8000-332 BCE. Oxford University Press, 0.
Tainter, J.A., 2006. Archaeology of overshoot and collapse. Annu. Rev. Anthropol. 35, 59–74.
Tallavaara, M., Jørgensen, E.K., 2020. Why are population growth rate estimates of past and present hunter–gatherers so different? Phil. Trans. Biol. Sci. 376, 20190708.
Tallavaara, M., Pesonen, P., 2020. Human ecodynamics in the north-west coast of Finland 10,000–2000 years ago. Quat. Int. 549, 26–35.
Thareani, Y., 2011. Tel 'Aroer: an Iron Age II Caravan Town and a Hellenistic and Early Roman Settlement in the Negev. Nelson Glueck School of Biblical Archaeology, Hebrew Union College-Jewish Institute of Religion, Jerusalem.
Thareani, Y., 2016. "The empire and the upper sea": assyrian control strategies along the southern levantine coast. Bull. Am. Sch. Orient. Res. 375, 77.
Thareani-Sussely, Y., 2007a. Ancient Caravanserais: an archaeological view from ‘aroer. Palest. Explor. Q. 123–141.
Thareani-Sussely, Y., 2007b. The 'Archaeology of the Days of Manasseh' reconsidered in the light of evidence from the Beersheba Valley. Palest. Explor. Q. 139, 69–77.
Timpson, A., Barberena, R., Thomas, M.G., Méndez, C., Manning, K., 2020. Directly modelling population dynamics in the South American Arid Diagonal using 14C dates. Phil. Trans. Biol. Sci. 376, 20190723.
Timpson, A., Colledge, S., Crema, E., Edinborough, K., Kerig, T., Manning, K., Thomas, M.G., Shennan, S., 2014. Reconstructing regional population fluctuations in the European Neolithic using radiocarbon dates: a new case-study using an improved method. J. Archaeol. Sci. 52, 549–557.
Titolo, A., Palmisano, A., 2025. From villages to empires: archaeological settlements of the south levant from the chalcolithic to the byzantine period. J. Open Archaeol. Data 13.
Utziel, J., Shai, I., 2010. The Settlement History of Tel Burna: Results of the Surface Survey, vol. 37, pp. 227–245. Tel Aviv.
Van der Plicht, J., 2004. Radiocarbon, the calibration curve and Scythian chronology: NATO Advanced Research Workshop on Impact of the Environments on Human Migration in Eurasia. In: Scott, E.M., Alekseev, A.Y., Zaitseva, G. (Eds.), Impact of the Environment on Human Migration in Eurasia. University of Groningen, Centre for Isotope Research, Amsterdam.
Webster, L.C., Wolff, S.R., Ortiz, S.M., Barbosa, M., Coyle, C., Arbino, G.P., Dee, M.W., Hua, Q., Jacobsen, G.E., 2023. The chronology of Gezer from the end of the late bronze age to iron age II: a meeting point for radiocarbon, archaeology egyptology and the Bible. PLoS One 18, e0293119.
Webster, L., Streit, K., Dee, M., Hajdas, I., Höflmayer, F., 2019. New Radiocarbon-based assessment Supports the Prominence of Tel Lachish during late Bronze age IB-IIA. Radiocarbon 61, 1711–1727.
Weiberg, E., Bevan, A., Kouli, K., Katsianis, M., Woodbridge, J., Bonnier, A., Engel, M., Finné, M., Fyfe, R., Maniatis, Y., Palmisano, A., Panajiotidis, S., Roberts, C.N., Shennan, S., 2019. Long-term trends of land use and demography in Greece: a comparative study. Holocene 29, 742–760.
Weiberg, E., Finné, M., 2018. Resilience and persistence of ancient societies in the face of climate change: a case study from late Bronze Age Peloponnese. World Archaeol. 50, 584–602.
Weiss, H., 2016. Global megadrought, societal collapse and resilience at 4.2-3.9 ka BP across the Mediterranean and west Asia. Past Global Change Magazine 24, 62–63.
Wilkinson, T.J., 2000. Regional approaches to mesopotamian archaeology: the contribution of archaeological surveys. J. Archaeol. Res. 8, 219–267.
Wilkinson, T.J., 2003. Archaeological Landscapes of the near East. University of Arizona Press, Tucson.
Wilkinson, T.J., Philip, G., Bradbury, J., Dunford, R., Donoghue, D., Galiatsatos, N., Lawrence, D., Ricci, A., Smith, S.L., 2014. Contextualizing early urbanization: settlement cores, early States and agro-pastoral strategies in the fertile Crescent during the fourth and third Millennia BC. J. World PreHistory 27, 43–108.
Williams, A.N., 2012. The use of summed radiocarbon probability distributions in archaeology: a review of methods. J. Archaeol. Sci. 39, 578–589.
Zertal, A., 1993. Fortified enclosures of the early Bronze Age in the Samaria Region and the beginning of urbanization. Levant 25, 113–125.
Zertal, A., 2003. The Province of Samaria (Assyrian Samerina) in the Late Iron Age (Iron Age III). In: Lipschits, O., Blenkinsopp, J. (Eds.), Judah and the Judeans in the Neo-Babylonian Period. Penn State University Press, pp. 377–412.
Zertal, A., 2004. The Manasseh Hill Country Survey, Volume 1: the Shechem Syncline. Brill, Leiden.
Zertal, A., 2007. The Manasseh Hill Country Survey, Volume 2: the Eastern Valleys and the Fringes of the Desert. Brill, Leiden.
Zertal, A., Bar, S., 2017. The Manasseh Hill Country Survey Volume 4: from Nahal Bezeq to the Sartaba. Brill, Leiden.
Zertal, A., Bar, S., 2019. The Manasseh Hill Country Survey Volume 5: the Middle Jordan Valley, from Wadi Fasael to Wadi ‘Aujah. Brill, Leiden.
Zertal, A., Mirkam, N., 2016. The Manasseh Hill Country Survey: Volume 3: from Nahal Iron to Nahal Shechem. Brill, Leiden.
Zimmermann, A., 2012. Cultural cycles in Central Europe during the Holocene. Quat. Int. 274, 251–258.
Ziv, B., Dayan, U., Kushnir, Y., Roth, C., Enzel, Y., 2006. Regional and global atmospheric patterns governing rainfall in the southern Levant. Int. J. Climatol. 26, 55–73.